Cellular/Molecular

Functional Cooperation between the IP_3 Receptor and Phospholipase C Secures the High Sensitivity to Light of *Drosophila* Photoreceptors *In Vivo*

Elkana Kohn, Ben Katz, Bushra Yasin, Maximilian Peters, Elisheva Rhodes, Rachel Zaguri, Shirley Weiss, and Baruch Minke

Departments of Medical Neurobiology, the Institute of Medical Research Israel-Canada, and the Edmond and Lily Safra Center for Brain Sciences, Faculty of Medicine of the Hebrew University, Jerusalem 91120, Israel

Drosophila **phototransduction is a model system for the ubiquitous phosphoinositide signaling. In complete darkness, spontaneous unitary current events (dark bumps) are produced by spontaneous single $G_q\alpha$ activation, while single-photon responses (quantum bumps) arise from synchronous activation of several $G_q\alpha$ molecules. We have recently shown that most of the spontaneous single $G_q\alpha$ activations do not produce dark bumps, because of a critical phospholipase Cβ (PLCβ) activity level required for bump generation. Surpassing the threshold of channel activation depends on both PLCβ activity and cellular [Ca^{2+}], which participates in light excitation via a still unclear mechanism. We show here that in IP_3 receptor (IP_3R)-deficient photoreceptors, both light-activated Ca^{2+} release from internal stores and light sensitivity were strongly attenuated. This was further verified by Ca^{2+} store depletion, linking Ca^{2+} release to light excitation. In IP_3R-deficient photoreceptors, dark bumps were virtually absent and the quantum-bump rate was reduced, indicating that Ca^{2+} release from internal stores is necessary to reach the critical level of PLCβ catalytic activity and the cellular [Ca^{2+}] required for excitation. Combination of IP_3R knockdown with reduced PLCβ catalytic activity resulted in highly suppressed light responses that were partially rescued by cellular Ca^{2+} elevation, showing a functional cooperation between IP_3R and PLCβ via released Ca^{2+}. These findings suggest that in contrast to the current dogma that Ca^{2+} release via IP_3R does not participate in light excitation, we show that released Ca^{2+} plays a critical role in light excitation. The positive feedback between PLCβ and IP_3R found here may represent a common feature of the inositol-lipid signaling.**

Key words: **Ca^{2+} release; *Drosophila*; IP_3 receptor; phospholipase C; photoreceptors; phototransduction**

Introduction

The phosphoinositide (PI) cascade is a diverse signaling pathway coupling a wide variety of surface membrane receptors to Ca^{2+} mobilization, enzyme activation, and ion channel activation and modulation, playing an important role in many biological systems (Berridge et al., 2000). PLC is a key element in the PI-signaling cascade, hydrolyzing phosphatidylinositol 4,5-bisphosphate (PIP_2) and generating two second messengers: IP_3 and DAG. IP_3 activates a Ca^{2+}-release channel located at the endoplasmic reticulum, the IP_3 receptor (IP_3R), resulting in the release of Ca^{2+} from internal stores (for review, see Berridge, 1993; Foskett et al., 2007; Taylor and Tovey, 2010). The major role of DAG is to activate PKC and to serve as an important source of downstream metabolites, including polyunsaturated fatty acids. These metabolites in *Drosophila* photoreceptors may be involved in a still unclear way in activation of the TRP channels (Chyb et al., 1999; Hofmann et al., 1999; Delgado et al., 2014).

Drosophila photoreceptors constitute an important genetic model for dissecting the PI-signaling (for review, see Montell, 1999; Minke and Cook, 2002; Pak and Leung, 2003; Hardie and Postma, 2008; Katz and Minke, 2009). In these cells, the absorption of photons by rhodopsin leads to G_q-dependent and PLCβ-mediated activation of the light-sensitive channels TRP (Montell and Rubin, 1989; Hardie and Minke, 1992; Minke and Selinger, 1992) and TRP-like (TRPL) (Phillips et al., 1992; Niemeyer et al., 1996). Although light-activated PLCβ generates large amounts of IP_3 (Devary et al., 1987), genetic elimination of the single IP_3R of *Drosophila* revealed normal phototransduction (Acharya et al., 1997; Raghu et al., 2000). The apparent lack of any effect on the light response by genetic elimination of the IP_3R in photoreceptors has been considered as crucial evidence against the involvement of IP_3-mediated Ca^{2+} release in light excitation, which has become the dogma in this field.

Received Sept. 23, 2014; revised Nov. 16, 2014; accepted Nov. 22, 2014.

Author contributions: E.K., B.K., M.P., and B.M. designed research; E.K., B.Y., E.R., R.Z., and S.W. performed research; E.K., B.K., B.Y., M.P., E.R., R.Z., and B.M. analyzed data; E.K., B.K., and B.M. wrote the paper.

This research was supported by grants from the National Eye Institute (NEI, R01 EY 03529), the Israel Science Foundation, and the Deutsch-Israelische Projektkooperation. Dr. Ben Katz is a postdoctoral fellow of Teva NNE and Edmond and Lily Safra Center for Brain Sciences. We thank Drs. Arthur Konnerth and Colin Taylor for useful comments on this manuscript and Drs. Moshe Parnas, Shahar Frechter, Shaya Lev, and Miguel Mantilla for critical reading of this manuscript. We also thank Dr. I. Bezprozvanny for the antibody against the IP_3R and Drs. François Payre and Armin Huber for the antibodies against dMoesin and PLC, respectively.

The authors declare no competing financial interests.

Correspondence should be addressed to Baruch Minke, Department of Medical Neurobiology, Faculty of Medicine, The Hebrew University, P.O. Box 12272, Jerusalem 91120, Israel. E-mail: baruchm@ekmd.huji.ac.il.

DOI:10.1523/JNEUROSCI.3933-14.2015

 0270-6474/15/352530-17$15.00/0

Table 1. Details of the various fly strains used in this study

Genotype	Description	Protein level (%WT)	Reference
w^{1118} (Abbreviation: WT)	White-eyed		
yw;P[GMR:Gal4, UAS:w-RNAi, y]/Cyo; P[UAS:IP_3R-RNAi, w] (Abbreviation: IP_3R-RNAi)	White-eyed transgenic fly with reduced expression level of IP_3R Stable line	~15% IP_3R (Fig. 1*A*)	P[UAS-IP_3R-RNAi] transgenic line no. 6486 from VDRC (Dietzl et al., 2007) yw;P[GMR:Gal4, UAS:w-RNAi, y]/CyO, a gift from A. Huber
Progenies of the cross: w;P[UAS:GCaMP6f]; X yw;P[GMR:Gal4, UAS:w-RNAi, y] (Abbreviation: wt/GCaMP6f)	Transgenic fly expressing the Ca^{2+} indicator GCaMP6f on a WT background Cross progeny		P[UAS-GCaMP6f] was obtained from Bloomington stock center #42747 (Chen et al., 2013)
Progenies of the cross: yw;P[GMR:Gal4, UAS:w-RNAi, y]/cyo; P[UAS:IP_3R-RNAi, w]; X P[UAS:GCaMP6f] (Abbreviation: GCaMP6f;IP_3R-RNAi)	White-eyed transgenic fly expressing GCaMP6f on background of reduced concentration of IP_3R Cross progeny		
Progenies of the cross: *$norpA^{H43}$;bw;st* X yw;P[y+,GMR-Gal4,UAS-]/CyO; P[UAS-RNAi-IP_3R,w] (Abbreviation: *$norpA^{H43}$;IP3R-RNAi*)	White-eyed transgenic fly expressing reduced concentration of IP_3R on white-eyed PLCβ mutant background Cross progeny	~79% PLCβ, ~15% IP_3R	
$norpA^{H43}$;bw;st (Abbreviation: *$norpA^{H43}$*)	White-eyed PLCβ mutant with Ser347Asn and Thr1007Ser mutations		A gift from W.L. Pak (Yoon et al., 2004)

Recent studies on *Drosophila* phototransduction investigated how phototransduction suppresses discrete electrical dark events (dark bumps) arising from spontaneous, single $G_q\alpha$ activation, while still maintaining single-photon sensitivity (Katz and Minke, 2012; Chu et al., 2013). Manipulations of PLCβ activity by mutations combined with modulations of cellular Ca^{2+} levels revealed that a critical level of PLCβ catalytic activity is required to initiate activation of the TRP and TRPL channels and hence to induce bump production. This threshold in channel activation enables suppression of most $G_q\alpha$-dependent dark noise, while maintaining the fidelity of single-photon sensitivity (Katz and Minke, 2012; Chu et al., 2013).

Establishment of new tools for the reduction of IP_3R concentration without causing the previously reported structural eye damage (Acharya et al., 1997; Raghu et al., 2000), together with new tools for measuring light-induced Ca^{2+} release from internal stores in *Drosophila*, have led us to reinvestigate the role of IP_3R in *Drosophila* light excitation. We show that reduced IP_3R level in *Drosophila* photoreceptors by RNAi or Ca^{2+} store depletion strongly reduced light sensitivity, linking Ca^{2+} release to light excitation. These results suggest that, in contrast to the current dogma, released Ca^{2+} plays a critical role in light excitation.

Materials and Methods

Fly stocks. Male flies were used for experiments on the *norpA* mutant. For all other experiments female flies were used because of their larger head size. All flies were raised at 24°C in a 12 h dark/light cycle. However, for whole-cell recordings vials with pupae were wrapped with aluminum foil and moved into a dark box 24 h before eclosion. For the details of the transgenic flies used in this study see Table 1.

Generation of transgenic flies with reduced IP_3R. P[UAS:IP_3R-RNAi,w] flies were crossed with a Gal4 strain to drive maximal suppression of IP_3R expression in the photoreceptors. The Gal4 expression was driven by the GMR promoter (P[GMR:Gal4,w]), which is a strong promoter and resulted in IP_3R suppression in the whole-eye imaginal disks (yw;P[GMR:Gal4, UAS:w-RNAi, y]/CyO; P[UAS:IP_3R-RNAi, w]; Weiss et al., 2012). These transgenic flies were white-eyed flies.

Western blots analysis. To measure a relative expression level of Rh1, $G_q\alpha$, PLCβ, and TRP proteins in photoreceptors, five fly heads were used as previously described (Katz and Minke, 2012). The blots were probed by anti-Rh1 (monoclonal; 1:1000 dilution, from Developmental Studies Hybridoma Bank, DSHB), anti-$G_q\alpha$ (polyclonal; 1:2000, from Dr. Z. Selinger), anti-PLCβ (polyclonal; 1:1000, from Dr. A. Huber), anti-TRP (monoclonal; 1:500, from DSHB), and anti-dMoesin antibodies (polyclonal; 1:10,000, from Dr. F. Payre). Relative protein amounts were quantified using ImageJ software (Abramoff et al., 2004). The density in each lane was corrected by the dMoesin signal (Chorna-Ornan et al., 2005) and calculated as a percentage of WT flies signals.

Since the IP_3R is expressed in all fly cells, isolated retinae were used to measure the level of IP_3R in the photoreceptors. Accordingly, 20–30 retinae from 1- to 2-d-old flies were isolated by the same dissection procedure used for whole-cell recordings and homogenized in a buffer solution (150 mM NaCl, 3 mM $MgCl_2$, 10% glycerol, and 50 mM HEPES, pH 7.4) and separated by 5% SDS-PAGE. The blots were probed with affinity-purified mouse anti-IP_3R (polyclonal, 1:100, see below).

Purification of IP_3R antibody. Biotin serum from rabbit immunized against the C terminal of *Drosophila* IP_3R (GGGGGCEQRKQKQRL-GLLNTTANSLLPFQ) custom synthesized (GL Biochem) was used for purification (Srikanth et al., 2004). The above peptide was conjugated to High Capacity NeutrAvidin Agarose Resin (Pierce) as follows: 2 ml of resin was loaded into a Bio-Rad Poly-Prep column and washed three times with 10 ml PBS, and then, 2 mg of peptide dissolved in 2 ml DDW was loaded on the column and incubated on a shaker at room temperature for 10 min and washed three times with 10 ml PBS. Serum was loaded on the column and incubated on a shaker for 1 h at 4°C. The column was centrifuged for 30 s at 500 *g* and washed three times with 10 ml PBS. Elution was done by loading 500 μl of 0.1 M glycine-HCl, pH 2.8, to the column; collected into 250 μl of Tris 1.5 M, pH 8.5; and the elution was repeated five times. The eluted antibody was dialyzed twice against 500 ml of PBS for 1 h using cellophane (14,000 kDa pore size), aliquoted, and kept at −20°C.

ERG and light stimulation. ERG recordings were applied to immobilized flies as described previously (Peretz et al., 1994a). Extracellular light responses were measured with standard glass micropipettes filled with Ringer's solution containing the following (in mM): 130 NaCl, 2 KCl, 5 $MgCl_2$, 2 $CaCl_2$, and 10 mM HEPES, pH 7.0, and introduced through the cornea into the extracellular matrix of the eye. Flies were grounded via a

Table 2. Extracellular solution for whole cell recordings

Solution name	NaCl (mM)	KCl (mM)	EGTA (mM)	TES (mM)	$MgCl_2$ (mM)	$CaCl_2$ (mM)	$SrCl_2$ (mM)	Tg (mM)	L-Proline (mM)	L-Alanine (mM)
Low Ca^{2+} Low Mg^{2+}	125	5	—	10	—	—	—	—	25	5
0 Ca^{2+} EGTA	125	5	0.5	10	4	—	—	—	25	5
1.5 mM Ca^{2+}	125	5	—	10	—	1.5	—	—	25	5
1.5 mM Sr^{2+}	125	5	—	10	—	—	1.5	—	25	5
1.5 mM Ca^{2+} + 4 mM Mg^{2+} + 10 μM Tg	125	5	—	10	4	1.5	—	0.010	25	5
1.5 mM Ca^{2+} + 4 mM Mg^{2+}	120	5		10	4	1.5	—	—	25	5

reference electrode that was placed on the thorax in a drop of electrode gel. Light from a xenon high-pressure lamp (PTI, LPS 220, operating at 50 W) or from 70 J photographic flash strobe passed via green filter (Balzers K-55 broad-band green filter) was delivered to the compound eye via a light guide. The green light, which is absorbed by states of fly Rh1, rhodopsin, and metarhodopsin, ensures strong activation of Rh1-rhodopsin and hence robust light excitation. At the same time the green light ensures an efficient metarhodopsin-to-rhodopsin photoconversion. Accordingly, the use of green light prevents the induction of the prolonged depolarizing afterpotential (PDA; for review see Minke, 2012), which constitutes a saturated response that extends in the dark for many minutes. Signals were amplified using a homemade amplifier. Currents were sampled at 1 kHz using an A/D converter (Digidata 1200; Molecular Devices), filtered below 0.5 kHz, and analyzed by the pClamp 8 software (Molecular Devices). The maximal luminous intensity at the eye surface was ~3.5 logarithmic intensity units above the intensity for a half-maximal response.

Whole-eye injection. An electrode filled with fly Ringer's solution (see above) supplemented with 25 mM EGTA was carefully broken on the eye surface and then introduced to the eye of an immobilized fly. Pressure injection (20 psi for 10 ms) was applied by Picoliter injector (PLI-90; Harvard/Medical Systems). A voltage artifact caused by the injection was visible (Fig. 2*C*). Control injection of Ringer's solution had no effect on the light response.

Anoxia. Anoxic state was obtained by blowing nitrogen (N_2) on the abdomen and thorax of immobilized flies. The onset and offset of N_2 application was accompanied by voltage artifact (Agam et al., 2000). Complete anoxia was typically achieved after ~200 s and was verified by applying two light pulses of maximal intensity. Complete anoxia was determined as failure to respond by >0.2 mV to the second light pulse.

Whole-cell recordings. The preparations and whole-cell recording experiments were performed in the dark except for dim red light, which was applied during the *Drosophila* eye dissection and whole-cell preparation as previously described (Hardie and Minke, 1992; Peretz et al., 1994b). Dissociated ommatidia were prepared from newly eclosed flies (<4 h post eclosion). Whole-cell voltage-clamp recordings were performed as described previously. For the various solutions used see also Tables 2 and 3. When low intracellular Ca^{2+} was needed, EGTA and $CaCl_2$ were added as noted, and the osmolarity was maintained by equal reduction of K gluconate. All calculations of free and EGTA-bound Ca^{2+} were calculated by MaxChelator version 8 (Patton et al., 2004). The pH of all solutions was 7.15. Recordings were made at 21°C using patch pipettes of 8–12 MΩ resistance, pulled from fiber-filled borosilicate glass capillaries. Junction potential was nulled before seal formation. Series resistance <30 MΩ was carefully compensated (>80%) for currents >100 pA. Membrane potential was clamped to −70 mV. Signals were amplified using an Axopatch-1D (Molecular Devices) patch-clamp amplifier. Currents were sampled at 5 kHz using an A/D converter (Digidata 1320a), filtered below 1 kHz, and analyzed by the pClamp 9.2 software (Molecular Devices). Light emitted from a xenon high-pressure lamp (Lambda LS; Sutter Instruments) was passed through an orange filter (Schott OG590 edge filter) and delivered to the ommatidia via the microscope's epi-illumination port to the objective lens. The orange light is mainly absorbed by Rh1-metarhodopsin (peak absorption ~570 nm) and it is not well absorbed by the Rh1-rhodopsin (peak absorption ~490 nm). These absorption properties of fly rhodopsin and metarhodopsin ensure maximal photoconversion of metarhodopsin to rhodopsin during orange lights and hence an efficient way to prevent induction of the PDA (Minke, 2012). The highly reduced absorption of the orange light by Rh1-rhodopsin prevents a robust activation of phototransduction, which usually leads to deterioration of the isolated ommatidia used for whole-cell recordings. A shutter (Lambda Smartshutter; Sutter Instruments) controlled by Master8 (A.M.P.I.) was used to control the duration of the orange light stimulus. Light was attenuated by a series of neutral density filters (Chroma) and was calibrated for effective photons per second of WT ommatidium by counting quantum bumps elicited by dim orange light. Light responses were recorded ~1 min after whole-cell formation, most of the responses were collected within 5 min of establishing the whole-cell configuration, unless a longer period was required (see Results). Responses were analyzed off-line using Clampfit 10.2 software (Molecular Devices).

Table 3. Intracellular solution for whole cell recordings

Solution name	D-Gluconic acid potassium salt (KGlu, mM)	$MgSO_4$ (mM)	TES (mM)	MgATP (mM)	NaGTP (mM)	EGTA	NAD (mM)	$CaCl_2$ (mM)
KGlu (0 mM $[Ca^{2+}]_i$)	140	2	10	4	0.4	—	1	—
KGlu + 1 mM EGTA (0 mM $[Ca^{2+}]_i$ + EGTA)	140	2	10	4	0.4	1.0	1	—
KGlu + 1 mM EGTA + 0.45 mM $[Ca^{2+}]_i$ (~300 nM free Ca^{2+})	140	2	10	4	0.4	1.0	1	0.45

Bump analysis. Quantum bumps were elicited by continuous dim orange illumination (Schott OG 590 edge filter). Bumps were detected and analyzed off-line using the "threshold detection" function in the Clampfit 10.2 software (Molecular Devices). To be detected as "bumps," they have to fulfill the following criteria: minimum peak amplitude of 3 pA, re-arm to 2 pA, minimum duration of 10 ms. To collect the large number of bumps necessary for a detailed statistical analysis, relatively long and stable recording periods were collected.

Ca^{2+} imaging. Flies genetically expressing GCaMP6f (Chen et al., 2013) were generated by crossing transgenic flies carrying the P[UAS: GCaMP6f] with transgenic flies carrying the P[GMR-Gal4] (see Table 1). The F1 progeny expressed the GCaMP6f protein specifically in the eye. The retinae were dissected and the ommatidia prepared as described for whole-cell recordings. Blue light from a green fluorescent filter set (ET-GFP; Chroma) served both for activation of the endogenous light response of the photoreceptor cell and excitation of the fluorescent indicator protein. The Ca^{2+} imaging sampling rate was either 160 Hz or 132.1 Hz, using a CCD camera (AM CCD IXONU885; Andor) for extracellular solution containing 1.5 mM Ca^{2+} or 0.5 mM EGTA, respectively. To estimate the relative change in $[Ca^{2+}]$, cellular fluorescence was sampled from the whole area of photoreceptor cell, including both the rhabdomere and cell body. The cell resting fluorescence was determined as the fluorescence of the average of the first three frames after the shutter was fully open (F_0). The delay in the light-induced increase of fluorescence after light onset reflecting the cell resting florescence was subtracted from the subsequent increase in cell fluorescence (ΔF). Data were analyzed using ImageJ software (Abramoff et al., 2004).

Electron microscopy. The initial procedure was similar for TEM and scanning electron microscopy (SEM) and both were performed as previ-

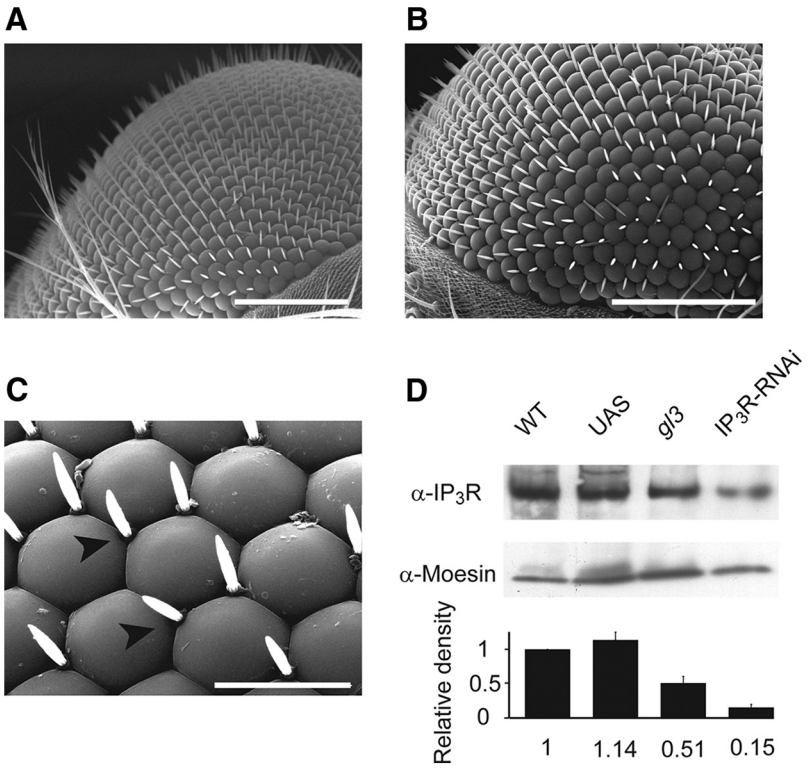

Figure 1. IP_3R-RNAi retinae show virtually normal eye morphology but reduced IP_3R expression levels. ***A–C***, SEM comparing eye of IP_3R-RNAi (***B***, ***C***) and WT flies (***A***). Scale bars: ***A***, ***B***, 100 μm; ***C***, 20 μm. Arrowheads point to corneal hairs. ***D***, Western blot analysis of isolated retinae (20–30 retinae for each lane) of IP_3R-RNAi fly using α-IP_3R. The expression levels of IP_3R in IP_3R-RNAi retinae are compared with its expression levels in isolated retinae of WT, P[UAS:IP_3R-RNAi] (UAS), and *gl3* mutant (lacking the photoreceptor cells). Relative protein amounts were quantified from band intensities. The density of each lane was divided by the density of α-Moesin (middle row) and calculated as a percentage of WT flies for each experimental run. Bottom, A histogram presenting the average of three independent experiments (mean ± SEM, $n = 3$); no significant difference was found between WT and UAS, (*t* test, $p = 0.140$), but a significant difference was found between WT and *gl3* (*t* test, $p = 0.037$) and between WT and IP_3R-RNAi (*t* test, $p = 0.0029$).

ously described (Weiss et al., 2012, TEM; Rubinstein et al., 1989, SEM). For SEM, flies were raised at complete darkness and heads were separated and bisected longitudinally from 3-d-old flies. Tissues including compound eyes were dissected out of the flies in fixative solution (fixation in 2.5% glutaraldehyde in 0.1 M cacodylate buffer with 5% sucrose added for 2 h) then diluted 1:1 and incubated overnight (4°C) and then washed again in cacodylate buffer 0.1 M × 4 × 15 min. Samples were then postfixed (2% OsO_4 in cacodylate buffer, pH 7.4) and washed ×4 10 min in cacodylate buffer 0.1 M and dehydrated through a graded series of ethanol. Samples following dehydration by ethanol series were dried in K850 Critical Point Drier (Quorum Technology) designed for use with liquid CO_2 replacing any water molecules in the specimen by ethanol. Then, the samples were spattered by gold and examined with EFI Quanta 200 SEM. For TEM, flies were raised at complete darkness and heads were separated and bisected longitudinally from flies at two ages: either newly eclosed or 3d old. Tissues including compound eyes were dissected out of the flies in fixative solution (5% glutaraldehyde and 0.1 M cacodylate buffer, pH 7.4) and incubated overnight. Samples were then postfixed (1% OsO_4 and 0.1 M cacodylate buffer, pH 7.4), dehydrated through a graded series of ethanol, and embedded in epoxy resin. Ultrathin sections were stained with uranyl acetate and lead citrate, observed with a Tecnai-12 TEM (FEI), and photographed with a charge-coupled MegaView 2 camera.

Results

Generation of transgenic flies with reduced expression level of IP_3R

The *Drosophila* genome encodes for a single IP_3R gene (Itp-r83A, CG1063). Genetic elimination of this gene causes lethality at the larval stage making it genetically challenging to evaluate its role in adult phototransduction *in vivo* (Acharya et al., 1997; Raghu et al., 2000). Therefore, we took an RNAi approach to knock down the IP_3R specifically in adult photoreceptor cells. Accordingly, P[UAS:IP_3R-RNAi] flies were crossed with a Gal4 strain driven by the glass multiple reporter (GMR) promoter (GMR:Gal4) to drive large suppression of IP_3R expression in the whole-eye imaginal disk (Weiss et al., 2012; see also Materials and Methods). We designated this transgenic fly as IP_3R-RNAi throughout this study. Using scanning electron microscopy, we found that in contrast to previous studies (Acharya et al., 1997; Raghu et al., 2000), the RNAi approach preserved the normal structure of the eye, except for a minor change in corneal hair arrangement (Fig. 1*A–C*). The eye morphology preservation most likely resulted from the use of the RNAi approach, which usually reduces but does not eliminate the target protein.

Western blot analysis from isolated retinae was used to determine the expression level of the IP_3R in the transgenic photoreceptor cells relative to WT or control flies, which have the same genetic background without hairpin expression (P[UAS:IP_3R-RNAi]) and negative control of *glass* mutant (gl^3), which lacks photoreceptor cells (Mealey-Ferrara et al., 2003). IP_3R-RNAi retinae showed ~85% reduction of IP_3R expression level relative to WT flies (Fig. 1*D*). The lower expression level of IP_3R in the mutant lacking photoreceptors gl^3 (~51%) relative to WT retina most likely reflects the fraction of IP_3R expression in nonphotoreceptor cells of the fly retina (Katz and Minke, 2009). Since IP_3R is expressed in most cells of the head, we used isolated retinae for the analysis shown in Figure 1*D* and not whole-head preparation. We also examined the expression levels of the major signaling proteins: Rh1, $G_q\alpha$, PLCβ, and TRP in IP_3R-RNAi heads relative to WT; P[UAS:IP_3R-RNAi]; and gl^3 flies, using an experimental procedure similar to Figure 1*D* but in whole-head preparation. The average of four to five independent experiments for each signaling protein revealed that no significant difference in the expression levels of Rh1 (*t* test, $p = 0.22$), $G_q\alpha$ (*t* test, $p = 0.23$), PLCβ (*t* test, $p = 0.13$), and TRP (*t* test, $p = 0.11$) were found between WT and IP_3R-RNAi flies, while no expression of any of the above signaling proteins was found in the *gl3* mutant (data not shown).

Low-expression level of IP_3R suppressed the ERG light response and this effect was exacerbated upon extracellular EGTA injection into the retina

It has been well established that a major role of the IP_3R is to mobilize intracellular Ca^{2+} upon PLC activation (Berridge, 1993; Taylor and Tovey, 2010). Therefore, a study of IP_3R function requires conditions that do not artificially change the resting Ca^{2+} level of cells. Caution should especially be implemented when studying *Drosophila* photoreceptor cells, where the IP_3-

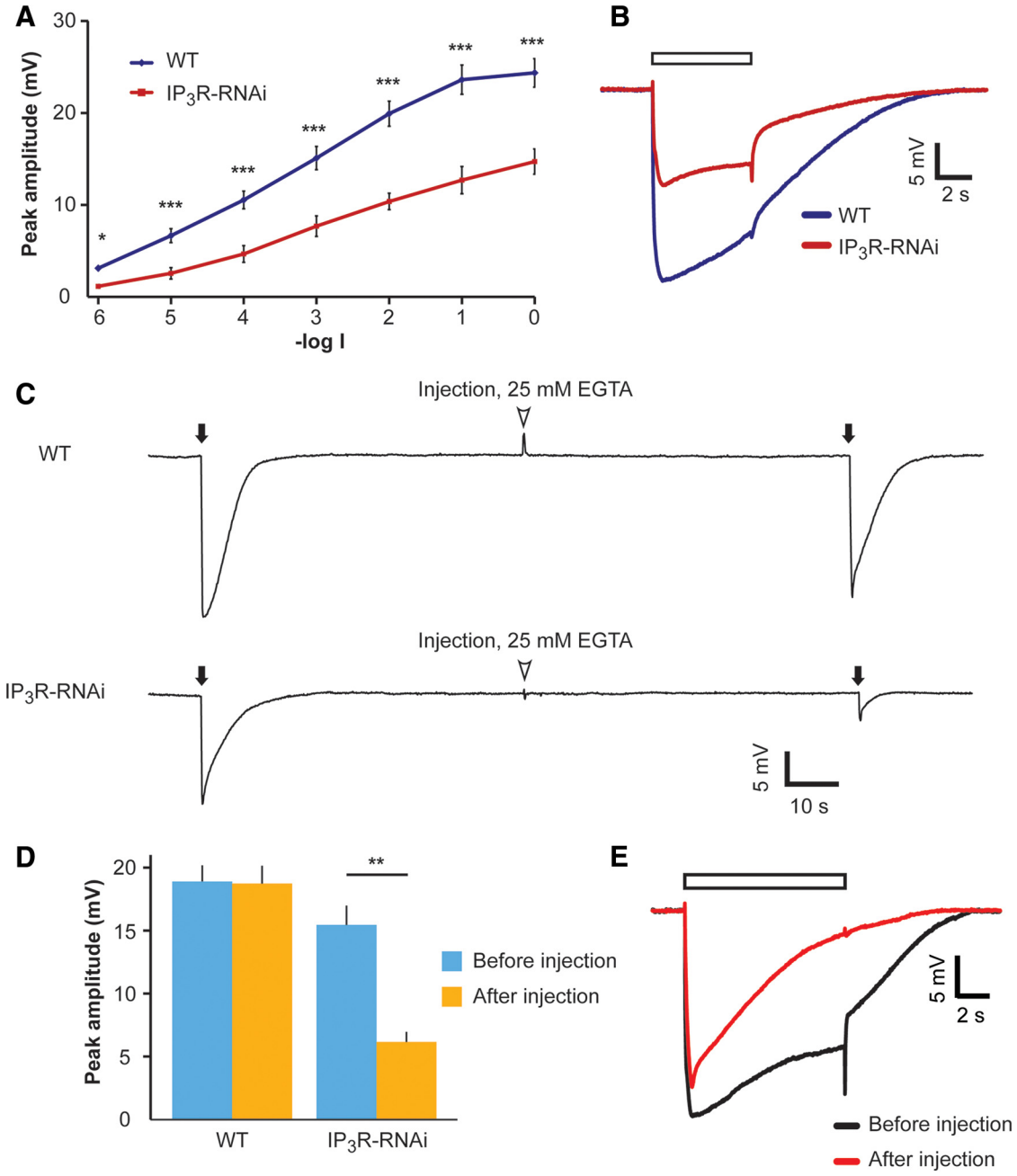

Figure 2. IP_3R-RNAi flies show reduced ERG response to light, which was further reduced at low external Ca^{2+}, *in vivo*. ***A***, Intensity–response (V-logI) curve of peak ERG response amplitudes. The different curves were measured from WT and IP_3R-RNAi flies in response to 5 s lights (mean ± SEM, *t* test, $*p < 0.05$, $***p < 0.001$; $n = 10$). ***B***, Representative ERG traces in response to a light pulse applied to IP_3R-RNAi and WT flies. ERG traces used in ***A*** at -log1 light intensity. The open box is the light monitor. ***C***, Reduced ERG amplitude in response to light flash at low extracellular Ca^{2+}. Top, Responses to brief saturated flashes (filled arrows) before and after pressure injection of EGTA-containing solution (arrowheads). Bottom, The same experimental paradigm was repeated in the IP_3R-RNAi fly. ***D***, A histogram summarizing the experiments presented in ***C***. A comparison of the response to light flash between WT and IP_3R-RNAi (mean ± SEM, *t* test, $p = 0.470$ and $p = 0.0016$ before and after EGTA injection, respectively; $n = 10$). ***E***, Superimposed ERG traces from a WT fly in response to prolonged light pulse (used in ***A*** and ***B***) before (black) and after (red) EGTA injection.

sensitive Ca^{2+} store is very small (Fig. 9; Katz and Minke, 2009). Previous studies on the IP_3R role used invasive techniques of recordings from *Drosophila* photoreceptors, which may affect the resting intracellular Ca^{2+} level. One study (Acharya et al., 1997) performed intracellular recordings with sharp electrodes, a technique that usually injures the penetrated cells, leading to a leak of external Ca^{2+} into the cell. The other study (Raghu et al., 2000) applied whole-cell patch-clamp recordings of isolated ommatidia, in which the pipette solution and hence intracellular solution was not buffered for Ca^{2+}, resulting in relatively high cytosolic Ca^{2+} concentration (estimated at several micromoles), relative to the measured *in vivo* cytosolic Ca^{2+} concentration (~160 nM; Hardie, 1996a). To avoid these difficulties, we initially studied the electrical response to light of photoreceptors with reduced IP_3R expression levels using the ERG, a noninvasive recording *in vivo*. The ERG is the summed electrical activity of the entire eye recorded *in vivo* (Peretz et al., 1994a). The IP_3R-RNAi flies displayed largely and significantly reduced amplitude of the ERG light response, relative to P[UAS:IP_3R-RNAi] flies (data not shown) or WT flies, at all light intensities tested (Fig. 2*A*,*B*).

Injection of EGTA into the retinal extracellular space is known to reduce the cytosolic Ca^{2+} concentration in intact photorecep-

tors by reducing the Ca^{2+} gradient between the cytosol and extracellular spaces (Peretz et al., 1994b; Agam et al., 2004). To reduce cytosolic $[Ca^{2+}]$ we injected Ringer's solution supplemented with 25 mM [EGTA] into the extracellular space of retinae of both WT and IP_3R-RNAi flies (Fig. 2*C*). The reduction in cellular Ca^{2+} in intact WT flies is known to convert the normal sustained response to prolonged lights into a transient response to prolonged lights (Hardie and Minke, 1992; Agam et al., 2004). To validate the effective reduction of cellular Ca^{2+} by the injected EGTA, at the end of each experiment we examined the shape of the ERG to sustained light (see representative example recorded in WT in Fig. 2*E*). Importantly, while the ERG peak amplitude of WT flies in response to intense, short (2 ms) flash light was slightly but not significantly affected by EGTA injection; the ERG response amplitude of the IP_3R-RNAi fly was largely and significantly suppressed (Fig. 2*C*,*D*). EGTA injection altered the time course of the WT ERG response to a brief intense flash consistent with the previous observation that highly reduced cellular Ca^{2+} induces a reduction in excitation efficiency as manifested in WT flies by the *trp* phenotype (Fig. 2*E*; Hardie and Minke, 1992; Agam et al., 2004). Therefore, the waveform of WT response following application of EGTA resembled the ERG response of IP_3R-RNAi, which is always reduced relative to WT, even before EGTA application (Fig. 2*C*).

The result of Figure 2 strongly suggests that reduced intracellular Ca^{2+} levels become a limiting factor in light excitation when combined with low expression of IP_3R.

Low-expression level of the IP_3R attenuated light-induced Ca^{2+} release from intracellular stores

To examine the notion that the reduced light response of IP_3R-RNAi flies and its further suppression at low intracellular Ca^{2+} arise from abnormally small light-induced release of Ca^{2+} from IP_3-sensitive stores, we measured Ca^{2+} release from intracellular stores using a genetically expressed Ca^{2+} indicator. To this end, we expressed the genetically encoded Ca^{2+} indicator protein GCaMP6f (Chen et al., 2013) in photoreceptor cells using the GMR:Gal4 driver. We measured light-induced intracellular Ca^{2+} elevation in dissociated ommatidia in a noninvasive manner, when GCaMP6f was expressed either on a WT background or on an IP_3R-RNAi background. Previous measurements of light induced Ca^{2+} elevation in *Drosophila* photoreceptors using membrane-impermeable Ca^{2+} indicators. These studies revealed robust light-induced increase in cellular Ca^{2+} above the dark level, a few milliseconds after light onset arising from Ca^{2+} influx via the TRP and TRPL channels (Peretz et al., 1994b; Ranganathan et al., 1994; Hardie, 1996a). Similarly, cells expressing GCaMP6f on a WT background bathed in 1.5 mM extracellular $[Ca^{2+}]$ ($[Ca^{2+}]_{out}$) also showed a fast increase in GCaMP6f fluorescence a few milliseconds after light onset due to Ca^{2+} influx (Fig. 3*A*, green curve). To prevent the masking of Ca^{2+} release from internal stores by the massive light-induced Ca^{2+} influx, we removed Ca^{2+} from the bathing extracellular solution. This was done by replacing the standard extracellular solution, which included 1.5 mM $[Ca^{2+}]_{out}$, by extracellular solution with no Ca^{2+} added ("0" Ca^{2+}), which was supplemented with 0.5 mM $[EGTA]_{out}$ as in similar previous studies (Peretz et al., 1994b; Ranganathan et al., 1994; Hardie, 1996a). The bath solution was replaced by at least 10 bath volumes of the 0 Ca^{2+} + 0.5 mM $[EGTA]_{out}$ solution during ~1 min before the Ca^{2+} measurements. Under these conditions, light-induced intracellular Ca^{2+} elevation arises solely from Ca^{2+} release from intracellular stores. In WT flies, elevation of cellular Ca^{2+} was observed at 0 external Ca^{2+} + 0.5 mM $[EGTA]_{out}$ (Fig. 3*A*, blue curve), showing a significantly slower kinetics relative to measurements under 1.5 mM $[Ca^{2+}]_{out}$ conditions (Fig. 3*A*, blue vs green curves). This relatively slow increase in fluorescence reflects Ca^{2+} release from stores. Importantly, under 0 external Ca^{2+} + 0.5 mM $[EGTA]_{out}$ conditions, the IP_3R-RNAi flies revealed an undetectable light-induced rise in cellular Ca^{2+} above the resting level during the initial ~200 ms after light onset (Fig. 3*A*, red curve). The delayed rise in cellular Ca^{2+} with slow kinetics relative to control (Fig. 3*A*, red curve) reflects a dramatic reduction in Ca^{2+} release from IP_3-sensitive stores in IP_3R-RNAi flies, consistent with reduced IP_3R in IP_3R-RNAi flies. The observed negative value of $\Delta F/F_0$ may reflect extrusion of basal cytosolic Ca^{2+} by the Na/Ca exchanger due to the perfusion of the 0 external Ca^{2+} + 0.5 mM $[EGTA]_{out}$ solution (Peretz et al., 1994b; Agam et al., 2004).

We next examined the effects of inhibiting the ER Ca^{2+} pump SERCA (Berridge et al., 2000; Wang et al., 2005). Inhibition of SERCA by thapsigargin (Tg) leads with time to deplete Ca^{2+} from the leaky internal stores and abolishes the response to intense light (Cook and Minke, 1999). Hence, application of Tg to WT ommatidia is expected to convert the kinetic of WT $[Ca^{2+}]$ changes to that of the IP_3R-RNAi flies. To examine this possibility, we performed Ca^{2+} imaging of intact photoreceptors of GCaMP6f on WT background in an experimental paradigm similar to that of Figure 3*A* (blue, red), except that the ommatidia were incubated in standard extracellular solution (1.5 mM $[Ca^{2+}]_{out}$) including 10 μM [Tg] for 15 min before the experiment, which was performed at 0 external Ca^{2+} + 0.5 mM $[EGTA]_{out}$ conditions (Fig. 3*C*,*D*). In ommatidia of GCaMP6f on WT background, Tg application largely reduced Ca^{2+} release from intracellular stores (compare Fig. 3*A*, blue, *C*, blue). In contrast to control ommatidia, in ommatidia of GCaMP6f on IP_3R-RNAi background Tg application had only a small effect of reduced Ca^{2+} release, but a similar slow kinetics indicative of highly reduced initial Ca^{2+} release was observed, similar to Ca^{2+} elevation without application of Tg (compare Fig. 3*A*, red, *C*, red). Longer (~20 min) application of Tg to WT photoreceptors completely eliminated intracellular Ca^{2+} elevation, probably because all Ca^{2+} stores were depleted of Ca^{2+} (Fig. 3*C*, green). The similarity of the kinetics of Ca^{2+} rise in Tg-treated WT and IP_3R-RNAi ommatidia supports our conclusion that reduced expression level of IP_3R leads to highly reduced light-induced Ca^{2+} release from IP_3-sensitive internal stores.

The observation of a similar slow rise of cellular Ca^{2+} after Tg treatment in flies with normal and with reduced level of IP_3R (Fig. 3*C*) suggests that the IP_3R is not involved in this slow Ca^{2+}-rising phase. This signal most likely reflects Ca^{2+} release from IP_3R-insensitive intracellular Ca^{2+} stores. Accordingly, the results suggest that the observed slow Ca^{2+} elevation in IP_3R-RNAi flies at 0 external Ca^{2+} was due to a small Ca^{2+} release via sparse IP_3R, which in turn may facilitate further Ca^{2+} release from ryanodine-sensitive stores (Walz et al., 1995; Arnon et al., 1997). Indeed, when the ommatidia of both WT and IP_3R-RNAi were perfused for 10 min with 5 mM ryanodine, Ca^{2+} stores were fully depleted, showing no increased fluorescence typical for fully depleted stores (data not shown) as observed when bathing the ommatidia for 20 min in Tg (Fig. 3*C*, green).

The results of Figure 3 showed that a highly reduced level of functional IP_3R in IP_3R-RNAi flies and Ca^{2+} store-depleted WT photoreceptors have highly reduced Ca^{2+} release. The results of Figures 1–3 demonstrate that reduced expression levels of IP_3R in IP_3R-RNAi transgenic flies cause reduction in light-induced

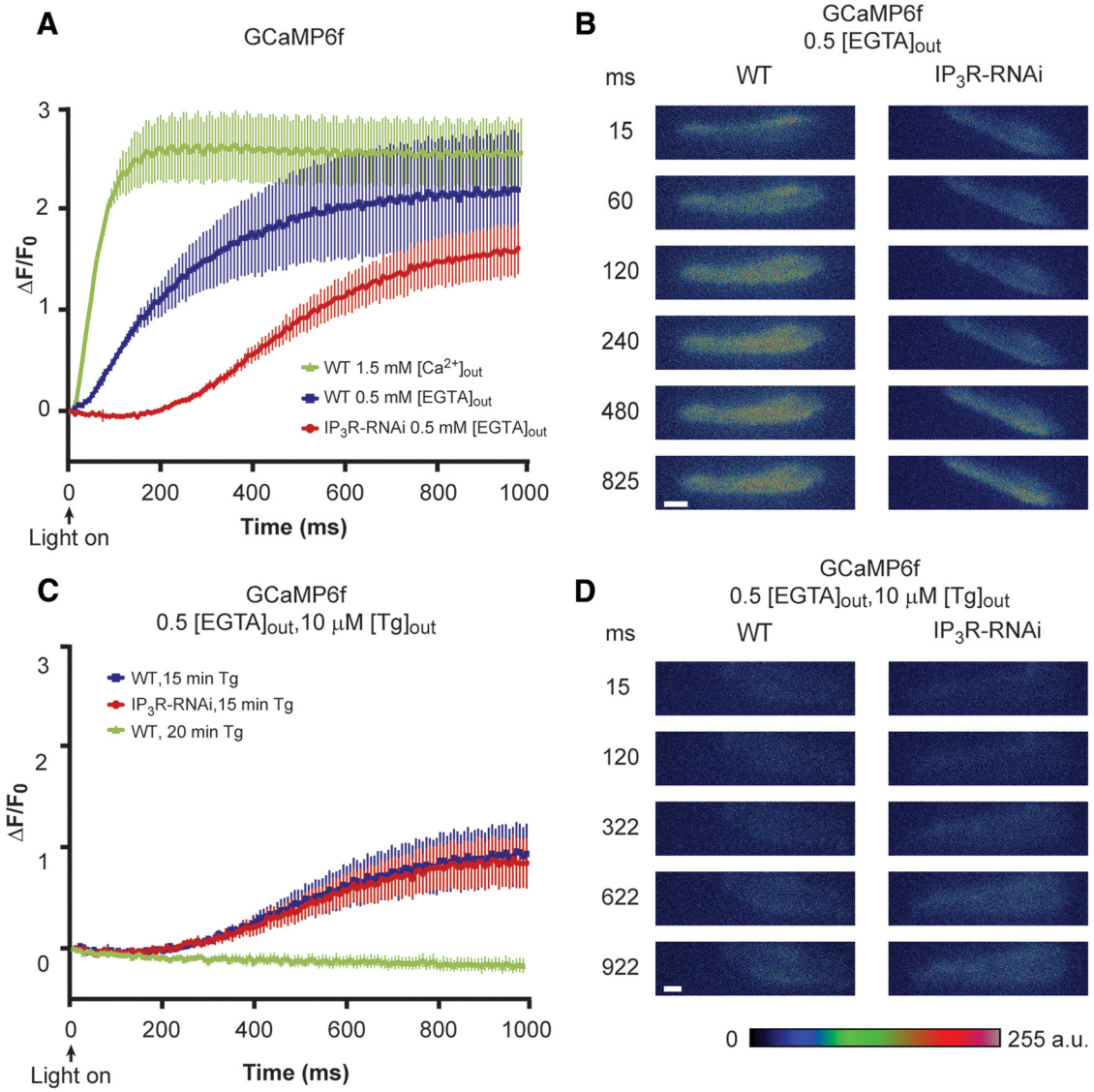

Figure 3. Reduced light-induced intracellular Ca^{2+} elevation in intact photoreceptors of IP_3R-RNAi flies as measured by GCaMP6f fluorescence. ***A***, Measurements of GCaMP6f fluorescence revealing the kinetics of light-induced increase in cytosolic [Ca^{2+}]. The ordinate plots $\Delta F/F_0$ (see Materials and Methods) as a function of time in GCaMP6f flies on WT background at 1.5 mM external [Ca^{2+}] (green) and at 0 (0.5 mM [EGTA]) external [Ca^{2+}] (blue) and in GCaMP6f flies on IP_3R-RNAi background at 0 (0.5 mM [EGTA]) external [Ca^{2+}] (red). The plotted curves are means ± SEM. To quantify the difference between the blue and red curves, we compared the difference in fluorescence intensity at 60 and 300 ms of the blue and red curves and found that IP_3R-RNAi flies expressing GCaMP6f at 0 extracellular Ca^{2+} (red) revealed a significant smaller increase of Ca^{2+} elevation in IP_3R-RNAi flies relative to WT flies (*t* test, $p = 0.0098$, $p = 0.0084$ at 60 and 300 ms after light onset, respectively; $n = 10$). Because of the high affinity of GCaMP6f to Ca^{2+} (K_d of ~170 nM) and the large Ca^{2+} influx at 1.5 mM $[Ca^{2+}]_{out}$, the Ca^{2+} indicator reached saturation at the time of maximal fluorescence and only the initial rise of the curves should be considered. ***B***, A time series of whole ommatidia images of control (WT background at 0 external Ca^{2+}) and IP_3R-RNAi ommatidia, showing the fluorescence of the GCaMP6f during light stimulation. Scale bar, 10 μm. ***C***, No difference was found between Ca^{2+} released from internal stores of control and IP_3R-RNAi after store depletion by Tg. Measurements of GCaMP6f fluorescence at 0 external Ca^{2+} (0.5 mM [EGTA]) following 15 min of prior incubation in standard extracellular solution (1.5 mM [Ca^{2+}]) including 10 μM Tg in WT (blue) and in IP_3R-RNAi backgrounds (red). Incubation of >20 min with Tg of ommatidia from GCaMP6f on WT background flies abolished the increase in fluorescence (green). Tg was also included in the 0 external Ca^{2+} solution during the fluorescent measurement ($n = 10$). ***D***, A time series of ommatidia images of control and IP_3R-RNAi at the conditions of ***C***, showing the fluorescence of the GCaMP6f during light stimulation. Scale bar, 10 μm.

Ca^{2+} release from intracellular stores and significantly reduced light-response amplitude *in vivo*.

Buffering of Ca^{2+} in the recording pipette solution suppressed the light response of IP_3R-RNAi photoreceptors

The results presented in Figures 2 and 3 conflict with previous studies (Acharya et al., 1997; Raghu et al., 2000). To understand the reason for this discrepancy, we examined the effect of Ca^{2+} buffering of the pipette solution (and hence intracellular Ca^{2+}) on the phenotype of IP_3R-RNAi flies. First, we measured the light-induced current (LIC) from IP_3R-RNAi photoreceptors using whole-cell patch-clamp recordings with standard intracellular solutions (i.e., without Ca^{2+} or Ca^{2+} buffer added to the pipette solution, which contained an estimated "nominal" level of several μM Ca^{2+}; Raghu et al., 2000). Under these conditions, the LIC amplitudes of WT and IP_3R-RNAi flies were similar, consistent with the previous studies (Acharya et al., 1997; Raghu et al., 2000; Fig. 4*A*, left, black vs red traces, *B*). Strikingly, when 1 mM [EGTA] was included in the pipette solution, the response to light of IP_3R-RNAi photoreceptors decreased by ~3-fold, while the response to light of WT flies increased by ~2-fold compared with the response at standard solution (Fig. 4*A*, right, black

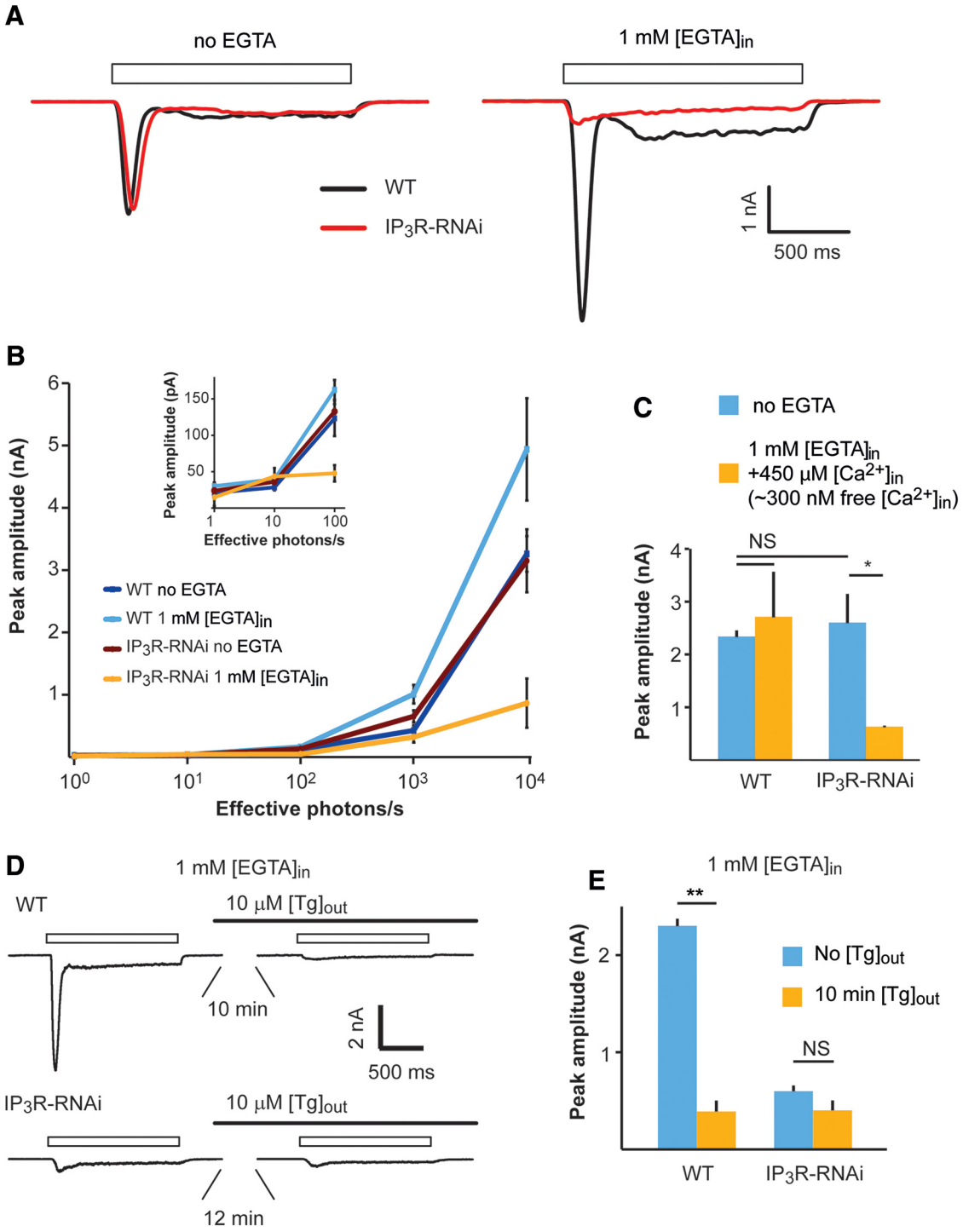

Figure 4. ***A–C***, Patch-clamp whole-cell recordings showing reduced responses to light of IP_3R-RNAi photoreceptors when Ca^{2+} is buffered by EGTA in the pipette solution. ***A***, Representative traces from whole-cell patch-clamp recordings with and without 1 mM [EGTA] added to the pipette solution. Open boxes represent the duration of light pulses. ***B***, Intensity–response relationship of WT and IP_3R-RNAi with and without 1 mM EGTA added into the pipette solution as indicated. Inset, The initial graph of ***B*** at higher magnification. ***C***, A histogram comparing light responses to a constant light intensity of WT and IP_3R-RNAi photoreceptors with standard intracellular solution and when the solution contained ~300 nM free Ca^{2+} (mean ± SEM, *t* test, $p = 0.045$; $n = 5$). ***D***, ***E***, Functional Ca^{2+} pump at the internal Ca^{2+} stores is required for normal light response while Ca^{2+} pump inhibition by Tg mimicked the phenotype of IP_3R-RNAi phenotype. ***D***, Representative whole-cell recordings of current traces obtained from WT (top) and IP_3R-RNAi photoreceptors (bottom), before and after prior incubation (10 min) of the cells in standard bath solution (1.5 mM [Ca^{2+}]) containing 10 μM [Tg]. Solid and open bars represent the time of Tg application and the light monitor, respectively. ***E***, Histograms comparing the peak amplitude of the light-induced current of WT and IP_3R-RNAi photoreceptors before and after 10 min of incubation with Tg (mean ± SEM, *t* test, $p = 0.0015$; $n = 5$).

traces vs red traces, *B*). EGTA is a slow Ca^{2+} buffer, which is known to have no direct effect on *Drosophila* light excitation (Hardie, 1995a; Agam et al., 2004). Thus, the enhanced light response of WT is a well known effect arising from removal of Ca^{2+}-dependent response inhibition (see below). Importantly, responses to light pulses of increasing intensities (R-logI curve) of IP_3R-RNAi photoreceptors showed highly reduced amplitudes when 1 mM [EGTA] was added to the

pipette solution (Fig. 4*B*). In contrast, no difference was observed in the R-logI curves between WT and IP_3R-RNAi flies when standard pipette solution (containing a few μM of Ca^{2+}) was used (Fig. 4*B*).

The "nominal" Ca^{2+} concentration of the standard pipette solution is unknown. To determine an upper limit for its possible physiological effect, we repeated the measurements of R-logI curves of Figure 4*B* with calculated 300 nM free [Ca^{2+}] in the pipette (standard intracellular solution containing 1 mM [EGTA] and 450 μM [Ca^{2+}]). Under this pipette solution, the response to light of IP_3R-RNAi photoreceptors was still reduced by ~3-fold relative to unbuffered pipette solution, while the response of WT photoreceptors was similar to the response with standard solution (Fig. 4*C*). Thus, the reduced response to light of IP_3R-RNAi photoreceptors relative to WT was still maintained at calculated pipette Ca^{2+} concentrations known to be above the estimated cytosolic [Ca^{2+}] level of *Drosophila* photoreceptors in the dark (~160 nM; Hardie, 1996a). The results of Figure 4, *A–C*, show that buffering the pipette Ca^{2+} to levels of <300 nM was sufficient to expose the phenotype of IP_3R-RNAi flies observed *in vivo*. As shown previously for WT flies, the intracellularly introduced EGTA buffer is too slow to inhibit light excitation directly. Therefore, the strong suppression of light excitation by EGTA in IP_3R-RNAi photoreceptors, but not in WT flies, strongly suggests a functional role of IP_3R in light excitation.

To support the above conclusion, we examined whether Tg is able to mimic the electrophysiological phenotype of IP_3R-RNAi fly in WT photoreceptors. To this end we measured the LIC in standard bath solution (1.5 mM [Ca^{2+}]) before and after incubation of the ommatidia in solution containing 10 μM [Tg], using recording pipette solution with 1 mM [EGTA]. Similar to a previous study (Cook and Minke, 1999), the response to light of WT photoreceptors decreased significantly (by ~85%) within 10 min after Tg application (Fig. 4*D*,*E*) and resembled in amplitude and waveform the LIC of IP_3R-RNAi photoreceptors. Furthermore, application of Tg to IP_3R-RNAi flies had virtually no effect on the response to light even 12–15 min after Tg application (Fig. 4*D*,*E*). This result shows that the phenotype of the IP_3R-RNAi fly was mimicked in WT flies by depleting the ER stores, but this depletion had no significant effect on IP_3R-RNAi photoreceptors. This result also demonstrates that the Tg-induced phenotype is due to depleting the ER stores and not due to some unknown and unspecific effect.

The rate but not amplitude of single-photon responses was reduced significantly in IP_3R-RNAi photoreceptors under Ca^{2+}-buffered pipette solution

To explore the mechanism underlying the reduction in response amplitude of IP_3R-RNAi photoreceptors under conditions of Ca^{2+}-buffered pipette solution, we measured single-photon responses (quantum bumps). *Drosophila* photoreceptors respond to single-photon absorption by a fast unitary voltage (or current) response called quantum bump (Wu and Pak, 1975), which sums to produce the macroscopic response to brighter light (Wong et al., 1982; Barash and Minke, 1994). When using standard pipette solution, we could not detect any significant difference between IP_3R-RNAi and WT photoreceptor in both quantum-bump rates at a given dim light (1.56 ± 0.10 bumps/s in WT, $n = 5$ and 1.50 ± 0.11 bumps/s in IP_3R-RNAi, $n = 5$; Fig. 5*A*, top, *B*) and mean bump amplitude (as derived from bump-amplitude distribution; Fig. 5*C–E*; 10.75 ± 0.18 pA, $n = 5$ and 11.29 ± 0.21 pA, $n = 5$ in WT and IP_3R-RNAi photoreceptors, respectively). However, under Ca^{2+}-buffered pipette solution the quantum-bump rate of IP_3R-RNAi photoreceptors was reduced by ~2-fold (0.67 ± 0.05 bumps/s, $n = 5$; Fig. 5*A*, bottom, *B*), while the quantum-bump rates of WT flies under the same conditions remained unchanged (1.55 ± 0.13 bumps/s, $n = 5$; Fig. 5*A*, bottom, *B*). Under pipette Ca^{2+}-buffered condition, the mean bump amplitude of both IP_3R-RNAi and WT as determined by the bump-amplitude distribution (Fig. 5*C*,*E*) increased by approximately the same extent, remaining similar in the two strains (Fig. 5*D*; 16.59 ± 0.16 pA, $n = 4$ and 18.44 ± 0.24 pA, $n = 4$ in WT and IP_3R-RNAi flies, respectively). The observed increase in the mean peak quantum-bump amplitude when EGTA was included in the intracellular solution (Fig. 5*A*, bottom, *D*) can be readily explained by removal of Ca^{2+}-mediated response suppression at the level of the TRP and TRPL channels (Henderson et al., 2000; Parnas et al., 2007).

In summary, we observed a significant reduction in quantum-bump rate in IP_3R-RNAi flies when pipette Ca^{2+} was buffered, reflecting a reduction in quantum efficiency of phototransduction (i.e., a reduction in the ability of absorbed photons to trigger quantum-bump production).

Reduced IP_3R expression levels combined with reduced catalytic activity of PLCβ strongly suppressed the response to light *in vivo*

To determine the site of action of the released Ca^{2+}, we examined whether Ca^{2+} release is required to enhance the activity of the light-sensitive PLCβ. To this end, we combined the IP_3R-RNAi transgene and a mutation resulting in low PLCβ catalytic activity. The $norpA^{H43}$ mutant has ~10-fold reduced catalytic activity of NORPA (fly PLCβ, CG3620) but nearly normal PLCβ expression level (Yoon et al., 2004; Katz and Minke, 2012). Similar to the IP_3R-RNAi fly, the intensity–response relationship (R-logI curve) of $norpA^{H43}$ measured by the ERG revealed reduced response to light and saturation of the response amplitude at lower light intensities relative to WT fly (Fig. 6*A*, middle curve). The figure shows that a much larger reduction of ERG amplitude was observed in the combined $norpA^{H43}$;IP_3R-RNAi fly relative to either $norpA^{H43}$ or IP_3R-RNAi flies in isolation (Figs. 2, 6). Accordingly, the maximal ERG amplitude was suppressed to ~64% of WT amplitude in both IP_3R-RNAi and $norpA^{H43}$ while it was suppressed to ~25% of WT amplitude in $norpA^{H43}$;IP_3R-RNAi flies. In addition, the sensitivity to dim lights was dramatically reduced by~1000-fold in $norpA^{H43}$;IP_3R-RNAi flies relative to ~10- and ~100-fold reduction in IP_3R-RNAi or $norpA^{H43}$ flies, respectively.

To examine if reduced cytosolic Ca^{2+} is a limiting factor in the suppression of the light response of the combined $norpA^{H43}$; IP_3R-RNAi fly, we induced Ca^{2+} influx in the dark via the TRP and TRPL channels to elevate cytosolic Ca^{2+}. This was done by applying anoxia to the $norpA^{H43}$;IP_3R-RNAi and $norpA^{H43}$ flies during ERG recordings. Anoxia is known to robustly open the TRP and TRPL channels and induce large Ca^{2+} influx into *Drosophila* photoreceptors in the dark *in vivo* (Agam et al., 2000). Therefore, we measured the amplitude of the ERG light response before and after application of anoxia to both $norpA^{H43}$ and $norpA^{H43}$;IP_3R-RNAi flies (Fig. 6*B–D*). In $norpA^{H43}$ flies the saturated ERG light-response amplitude after application of anoxia was slightly but significantly reduced relative to control (Fig. 6*B–D*; *t* test, $p = 0.0014$). In contrast, in the $norpA^{H43}$;IP_3R-RNAi flies the maximal ERG light-response amplitude was increased significantly after application of anoxia (Fig. 6*C*; *t* test, $p =$

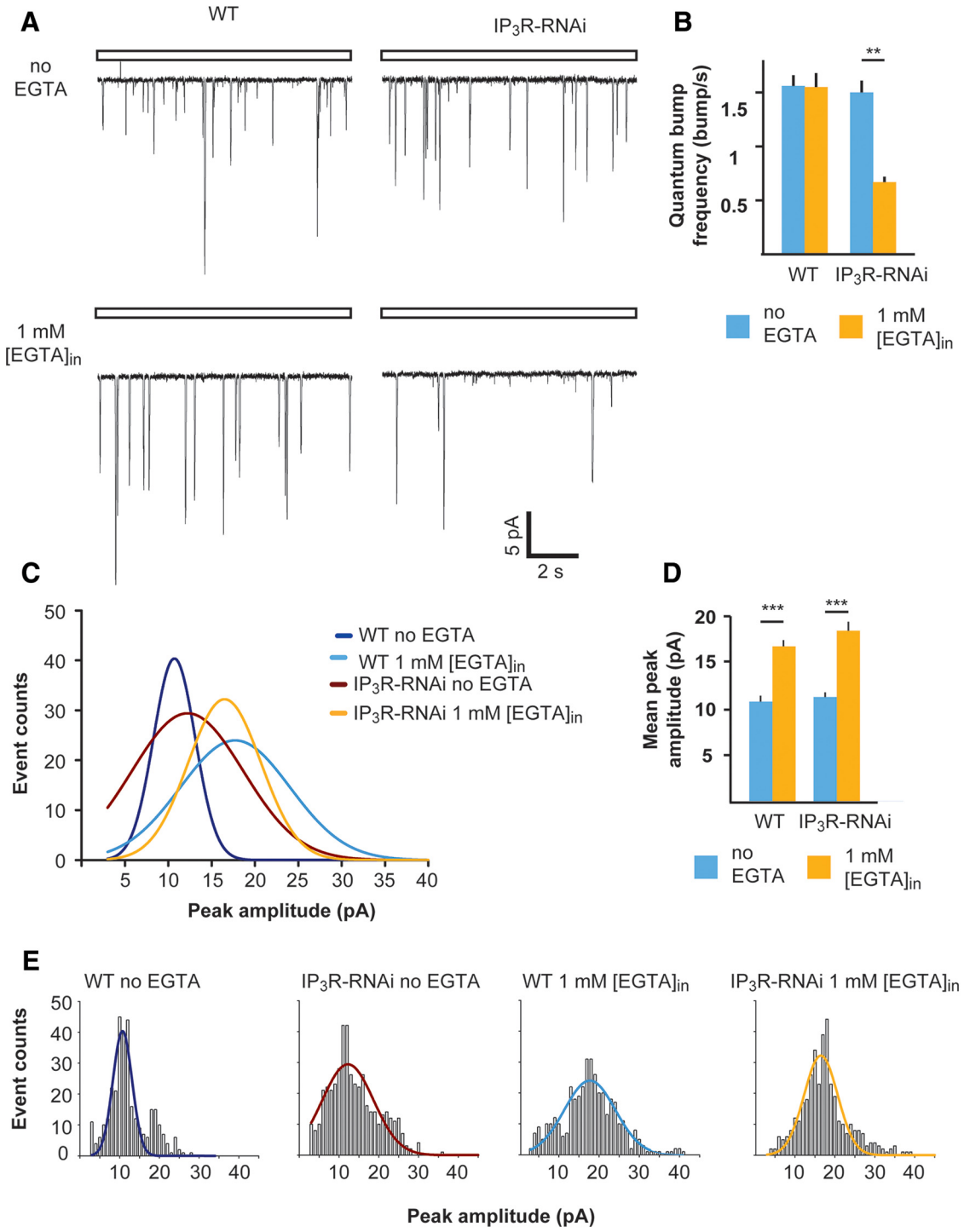

Figure 5. The frequency but not amplitude of single-photon responses was reduced significantly in IP_3R-RNAi flies compared with WT flies when the pipette solution was buffered with EGTA. ***A***, Representative traces of unitary current responses to single photons (quantum bumps) of WT and IP_3R-RNAi ommatidia recorded with standard pipette solution (top) or with 1 mM [EGTA] added (bottom). ***B***, A histogram comparing the quantum-bump frequency of WT and IP_3R-RNAi photoreceptors with or without EGTA in the recording pipette (mean ± SEM, *t* test, $p = 0.0058$; $n > 300$ bumps for each column, $n = 4$). ***C***, Distributions of quantum-bump amplitudes. The Gaussians that fit the histograms of quantum-bump amplitude distribution in ***E*** ($n > 300$ for each histogram, with and without EGTA in the pipette solution). ***D***, A histogram comparing the mean quantum-bump amplitudes of WT and IP_3R-RNAi with or without EGTA in the recording pipette (mean ± SEM, *t* test, $p = 0.00038$, $p = 0.00078$, for WT and IP_3R-RNAi flies, respectively) as derived from bump-amplitude distributions of ***E***. ***E***, Histograms of bump-amplitude distribution with the fitted Gaussians presented in ***C***.

0.00035). The increase in cellular Ca^{2+} by anoxia (Agam et al., 2000) and the partial rescue of reduced ERG amplitude of the $norpA^{H43}$;IP_3R-RNAi by anoxia, suggests that cellular Ca^{2+} was a limiting factor in light-response suppression of the $norpA^{H43}$; IP_3R-RNAi flies.

Whole-cell measurements show robust suppression of the response to light by combined reduction of IP_3R expression levels and PLCβ catalytic activity

To further support the conclusion derived from *in vivo* ERG experiments that Ca^{2+} was the limiting factor in light-response

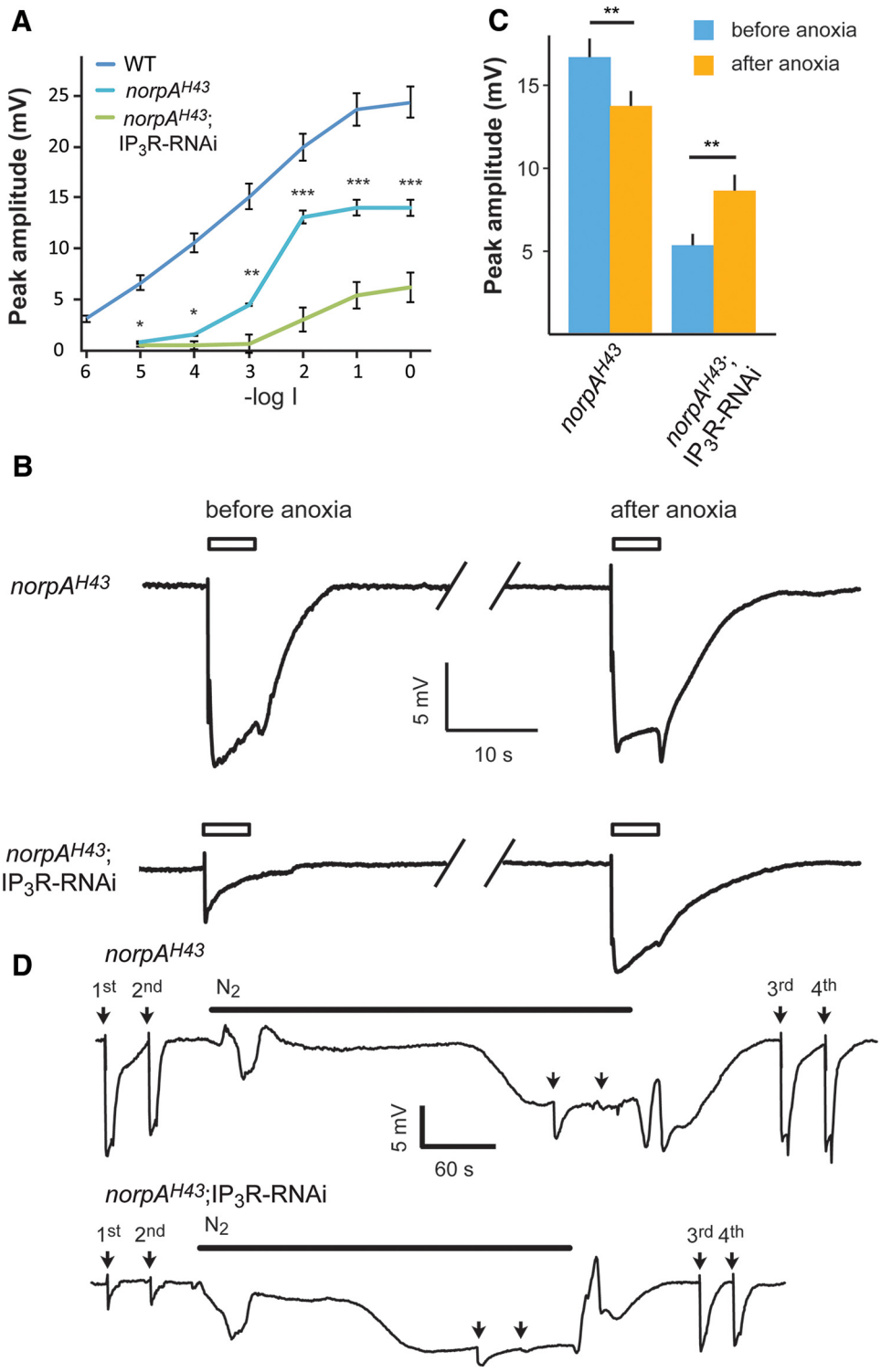

Figure 6. Ca^{2+} is a limiting factor, which determines the maximal ERG amplitude when reduced IP_3R levels were combined with reduced catalytic activity of PLCβ. ***A***, Intensity–response relationship of peak ERG responses to increasing intensities of light stimulations of WT (redrawn from Fig. 2), $norpA^{H43}$, and $norpA^{H43}$;IP_3R-RNAi flies. ***B***, Traces of ERG recordings of $norpA^{H43}$ and $norpA^{H43}$;IP_3R-RNAi in response to maximal intensity light pulses (open bar) before and after application of anoxia (see ***D*** below), which is known to robustly increase cellular Ca^{2+}. ***C***, A histogram comparing the peak amplitude of the ERG light responses of $norpA^{H43}$ and $norpA^{H43}$;IP_3R-RNAi before and after anoxia (mean ± SEM, *t* test, $p = 0.0014$ and $p = 0.00035$ for $norpA^{H43}$ and $norpA^{H43}$;IP_3R-RNAi, respectively; $n = 10$). ***D***, Traces showing the entire experiments from which the ERG traces of ***B*** were taken. Traces of prolonged ERG recordings of $norpA^{H43}$ (top trace) and $norpA^{H43}$;IP_3R-RNAi (bottom trace) in response to maximal intensity light pulses (arrows) followed by N_2 application. Anoxia was obtained by blowing N_2 on the intact fly as indicated by the horizontal line. The additional light pulses (3rd and 4th), tested the effects of cellular Ca^{2+} elevation by the anoxia on the ERG. The amplitudes of the ERG responses to the first and the third light pulses in each trace should be compared. The light pulses applied during anoxia (2 unmarked arrows) induced only very small light responses because most TRP and TRPL channels were already open by the anoxia.

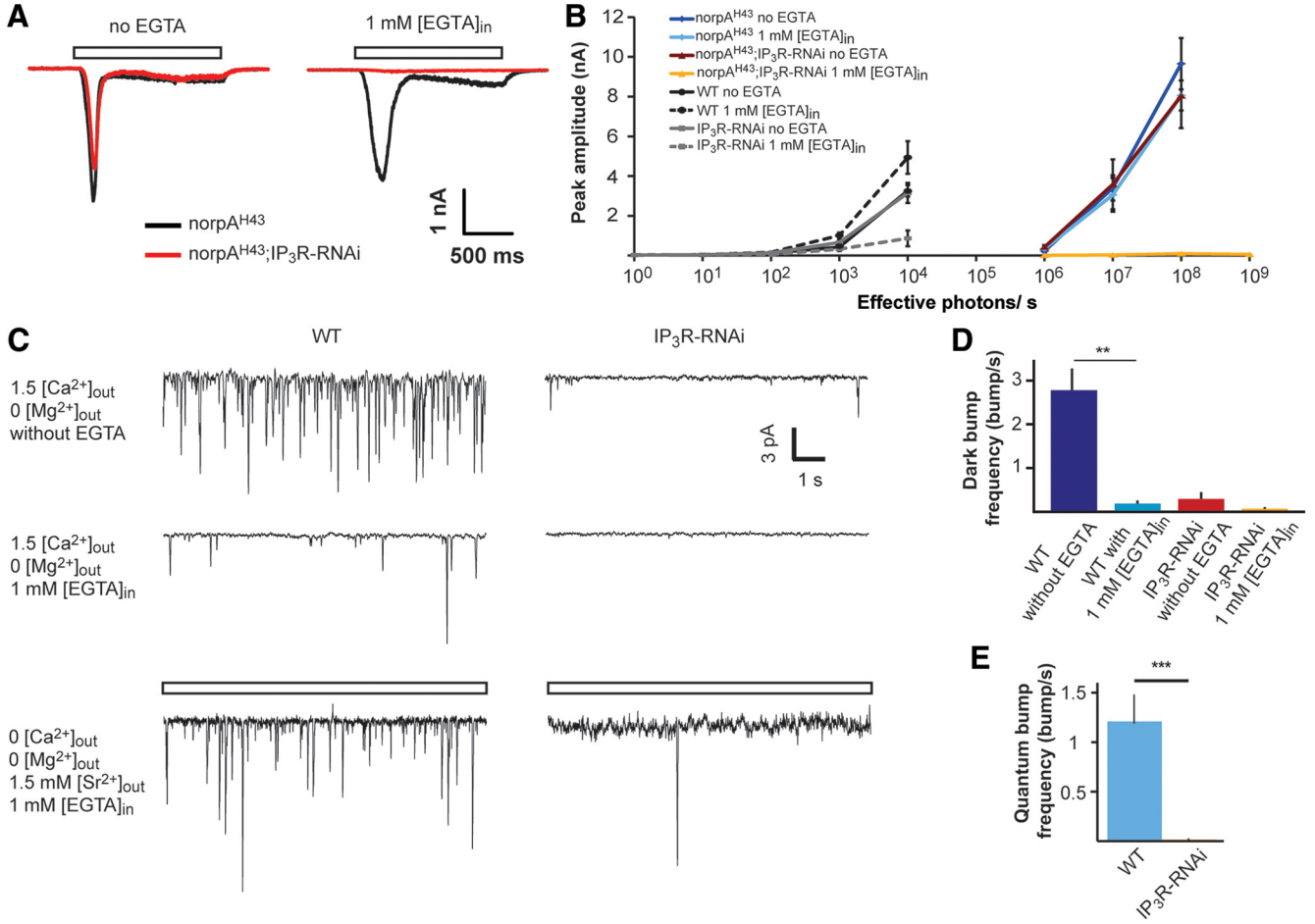

Figure 7. Synergistic effect on the response to light between reduced IP_3R level and reduced catalytic activity of PLCβ as revealed by whole-cell recordings. ***A***, Representative traces showing whole-cell patch-clamp recordings from *norpA*^{H43} (black) and *norpA*^{H43};IP_3R-RNAi (red) with and without 1 mM [EGTA] added into the standard pipette solution. ***B***, Intensity–response relationship of *norpA*^{H43} (redrawn from Fig. 4) and *norpA*^{H43};IP_3R-RNAi with and without EGTA added into the pipette as indicated. ***C***, ***D***, Dark-bump production was virtually abolished in IP_3R-RNAi photoreceptors (***C***, top and middle left traces). Representative traces showing dark bumps of WT fly recorded for 1 min at 1.5 mM external [Ca^{2+}] while Mg^{2+} was omitted from the bath solution. The dark bumps were recorded without (top) or with 1 mM [EGTA] (middle) in the pipette solution. The paradigm of the left traces was repeated in IP_3R-RNAi fly (***C***, top and middle right traces). ***D***, A histogram presenting dark-bump frequency during 1 min recordings in WT and IP_3R-RNAi photoreceptors at the conditions of ***C*** (mean ± SEM, *t* test, $p = 0.00598$, $n = 5$; ***C***, bottom line and ***E***). Quantum-bump production of IP_3R-RNAi photoreceptors was virtually abolished when extracellular Ca^{2+} was replaced by Sr^{2+} and Ca^{2+} was buffered in the intracellular pipette solution (***C***, bottom left). Traces showing quantum bumps of WT in response to dim light of 1.5 effective photons/s (open box) recorded for 1 min when extracellular Ca^{2+} was replaced by 1.5 mM $[Sr^{2+}]_{out}$, Mg^{2+} was omitted from the bath solution, and 1 mM [EGTA] was included in the pipette solution. Bottom right, The paradigm of the bottom left trace was repeated in IP_3R-RNAi fly. ***E***, A histogram presenting quantum-bump frequency during 1 min recordings in WT and IP_3R-RNAi photoreceptors when extracellular Ca^{2+} was replaced by Sr^{2+} (mean ± SEM, *t* test, $p = 0.00013$; $n = 5$).

suppression of the *norpA*^{H43};IP_3R-RNAi fly, we applied whole-cell recordings to these photoreceptors in a similar experimental paradigm of Figure 4. The measurements of the R-logI curve of the *norpA*^{H43} mutant and *norpA*^{H43};IP_3R-RNAi photoreceptors when no EGTA was added to the pipette solution were similar but strongly shifted to higher levels of light intensities (Fig. 7*A*,*B*, dark red curve) relative to WT flies (redrawn from Fig. 4). Strikingly, the R-logI curve of *norpA*^{H43};IP_3R-RNAi photoreceptors measured when EGTA was included in the recording pipette was virtually eliminated (Fig. 7*A*,*B*, yellow curve) and no response to light was observed at all light intensities, even when the light intensity was further increased by 10-fold (Fig. 7*B*).

In summary, in *norpA*^{H43};IP_3R-RNAi photoreceptors in which reduced catalytic activity of PLCβ was combined with reduced Ca^{2+} release from IP_3-sensitive stores, when EGTA was included in the pipette, the light response was virtually abolished. This result indicates that PLCβ catalytic activity is a site of action of Ca^{2+} release through the IP_3R. These data further suggest that there is a functional cooperation between the IP_3R and PLCβ.

Spontaneous dark bumps were virtually abolished in IP_3R-RNAi photoreceptors

To support the notion of functional cooperation between IP_3R and PLCβ we measured spontaneous production of unitary current signals (dark bumps), which are highly sensitive to $G_q\alpha$-dependent PLCβ catalytic activity and cellular Ca^{2+} levels (Katz and Minke, 2012). In *Drosophila* photoreceptors, dark activation of single $G_q\alpha$ molecules occurs spontaneously and produces dark bumps (Hardie et al., 2002; Elia et al., 2005; Katz and Minke, 2012). When Ca^{2+} was omitted from the extracellular solution, dark bumps were virtually absent (Katz and Minke, 2012). Consistent with previous findings, inclusion of 1 mM [EGTA] in the pipette solution largely reduced dark-bump frequency in WT photoreceptors (Fig. 7*C*, middle left, *D*). In contrast, normal quantum-bump frequency of WT photoreceptors was observed when 1 mM [EGTA] was included in the recording pipette (Fig. 5*A*,*B*). This difference between dark bumps and quantum bumps was explained by a model as follows. Unlike single $G_q\alpha$-activated dark bumps,

single-photon activation synchronized approximately five relatively low activity levels of single PLCβ molecules under low Ca^{2+} conditions and thus exceeded the minimal level of integrated PLCβ activity required for bump generation. This synchronous channel activation underlies quantum-bump production, even under low Ca^{2+} conditions (Katz and Minke, 2012). Strikingly, in IP_3R-RNAi photoreceptors a large reduction of dark-bump production was observed even without including EGTA in the recording pipette, while dark-bump production was virtually abolished when 1 mM [EGTA] was included in the pipette solution (Fig. 7*C*, middle right, *D*). Since dark-bump production critically depends on cellular Ca^{2+} level and PLCβ catalytic activity (Katz and Minke, 2012), the observed reduction in dark-bump production in IP_3R-RNAi photoreceptors indicates that Ca^{2+} release from internal stores is needed to increase PLC activity above the critical level of PLCβ catalytic activity required for bump generation (but also see model in Fig. 8 and Discussion).

Activated PLC failed to produce quantum bumps when extracellular Ca^{2+} was replaced by Sr^{2+} and Ca^{2+} was buffered in the intracellular pipette solution

Additional evidence for functional cooperation between the IP_3R and PLCβ was based on exploiting the ability of Sr^{2+} to substitute Ca^{2+} as charge carrier and regulator of the TRP/TRPL channels but not as a facilitator of PLCβ catalytic activity. TRP, TRPL, and IP_3R channels are all permeable to Sr^{2+}, which is frequently used to replace Ca^{2+} (Katz and Minke, 2012). We recorded quantum bumps from WT and IP_3R-RNAi photoreceptors in extracellular solution containing 1.5 mM [Sr^{2+}] while no Ca^{2+} or Mg^{2+} was added (0 $[Ca^{2+}]_{out}$, 0 $[Mg^{2+}]_{out}$, and 1.5 mM $[Sr^{2+}]_{out}$). Mg^{2+} was omitted from the solution as it inhibits the TRP and TRPL channels in the absence of Ca^{2+} and slows the response kinetics (Katz and Minke, 2012). The quantum-bump frequency of WT flies was slightly decreased when Ca^{2+} was substituted with Sr^{2+} in the extracellular solution and EGTA was included in the pipette. Also, quantum-bump amplitude was largely reduced (Figs. 5, 7*C*, bottom). The measurements revealed that in IP_3R-RNAi photoreceptors, the quantum bumps virtually disappeared (Fig. 7*C*, bottom right, *E*). In most cells, a minimal rate of 0.017 quantum bumps/s was observed, showing dramatic reduction in quantum-bump rate relative to similar experimental paradigm, but when bath solution contained 1.5 mM [Ca^{2+}] (showing a rate of 1.2 quantum bump/s; Fig. 5*B*). The interpretation of this result is that in the absence of extracellular Ca^{2+}, only store Ca^{2+} is available for quantum-bump production. Therefore, in IP_3R-RNAi photoreceptors, the reduced release of Ca^{2+} from the stores was not sufficient for TRP/TRPL channel activation and bump production was suppressed. In contrast, in WT photoreceptors activation of PLCβ induced Ca^{2+} release from the internal stores, which was sufficient for TRP/TRPL channel activation and quantum-bump production, albeit with reduced amplitude as found for the *norpA*^{H43} mutant (Katz and Minke, 2012). This experiment thus indicates that the functional cooperation between PLCβ and the IP_3R is highly dependent on intracellular [Ca^{2+}] and Ca^{2+} release from internal stores via IP_3R. Accordingly, quantum-bump production is dramatically attenuated when no Ca^{2+} is released from IP_3-sensitive stores and Ca^{2+} was substituted with Sr^{2+} in the extracellular solution.

Discussion

IP_3R has a critical role in light excitation of *Drosophila* photoreceptors

In this study, in *vivo* light-response suppression was accompanied by reduced Ca^{2+} release from IP_3-sensitive stores. In addition, the rate of spontaneously produced dark bumps, which is highly sensitive to $G_q\alpha$-dependent PLCβ catalytic activity and cellular Ca^{2+} level, was virtually abolished in IP_3R-deficient photoreceptors. This dark-bump elimination indicates that the suppressed Ca^{2+} release from IP_3-sensitive stores underlies the suppressed catalytic activity of PLCβ, leading to suppressed light response in IP_3R-deficient photoreceptors. Further evidence that the suppressed light response arises from inhibition of Ca^{2+} release from IP_3-sensitive stores came from blocking the Ca^{2+} pump by Tg, which mimicked the phenotype of the IP_3R-deficient photoreceptors in WT flies. The above findings indicate that IP_3R-mediated Ca^{2+} release has a critical role in light excitation of *Drosophila* photoreceptors. The combination of the PLCβ mutant *norpA*^{H43} with IP_3R-deficient photoreceptors, which synergistically suppressed the light response, strongly suggests that there is functional cooperation between the IP_3R and PLCβ in generation of the light response.

Functional cooperation between the IP_3R and PLCβ via the released Ca^{2+}

It has been previously shown that an increase in cytosolic Ca^{2+} participates in light excitation as evidenced by enhancement of the light response following photo release of caged Ca^{2+} at the rising phase of the light response (Hardie, 1995b). The target of Ca^{2+} action has not been entirely resolved. PLCβ is an important target for Ca^{2+} action and the regulation of its catalytic activity by Ca^{2+} has been thoroughly investigated. These studies showed that the positive charge of Ca^{2+} is used to counterbalance local negative charges formed in the active site during the course of the catalytic reaction. Accordingly, Ca^{2+} performs electrostatic stabilization of both the substrate and the transition state, thus providing a twofold contribution to lower the activation energy of the enzyme reaction (Essen et al., 1997).

The following model explains how functional cooperation between the IP_3R and PLCβ via the released Ca^{2+} operates and secures quantum-bump production: absorption of a single photon, which induces activation of several PLCβ molecules (Hardie et al., 2002; Katz and Minke, 2012), is initially insufficient at resting Ca^{2+} levels to reach the critical level of PLCβ activity required for TRP/TRPL channel activation. Nevertheless, the IP_3 molecules produced by the given PLCβ activity are able to activate the nearby IP_3Rs, mobilize Ca^{2+} from the stores, and elevate PLCβ activity above the threshold required for TRP/TRPL channel activation (Fig. 9*C*; Katz and Minke, 2012). In addition, the released Ca^{2+} may also reduce the threshold of TRP/TRPL channel activation and allow bump generation (Hardie, 1995b; Chu et al., 2013). According to this model, the following enzymatic reactions may explain our findings (Fig. 9*C*). Each $G_q\alpha$-activated PLCβ has low catalytic activity due to the relatively low ($<$160 nM) resting Ca^{2+} concentration in the cytosol (Hardie, 1996b). In addition, each activated PLCβ remains active for only a short (approximately several tens of milliseconds) time due to the GTPase-activating protein activity of PLCβ that causes a rapid hydrolysis of $G_q\alpha$-GTP followed by inactivation of PLCβ (Cook et al., 2000). The initial low catalytic activity of PLCβ is apparently below the threshold required for activation of the TRP and TRPL channels (Katz and Minke, 2012), but this low activity still

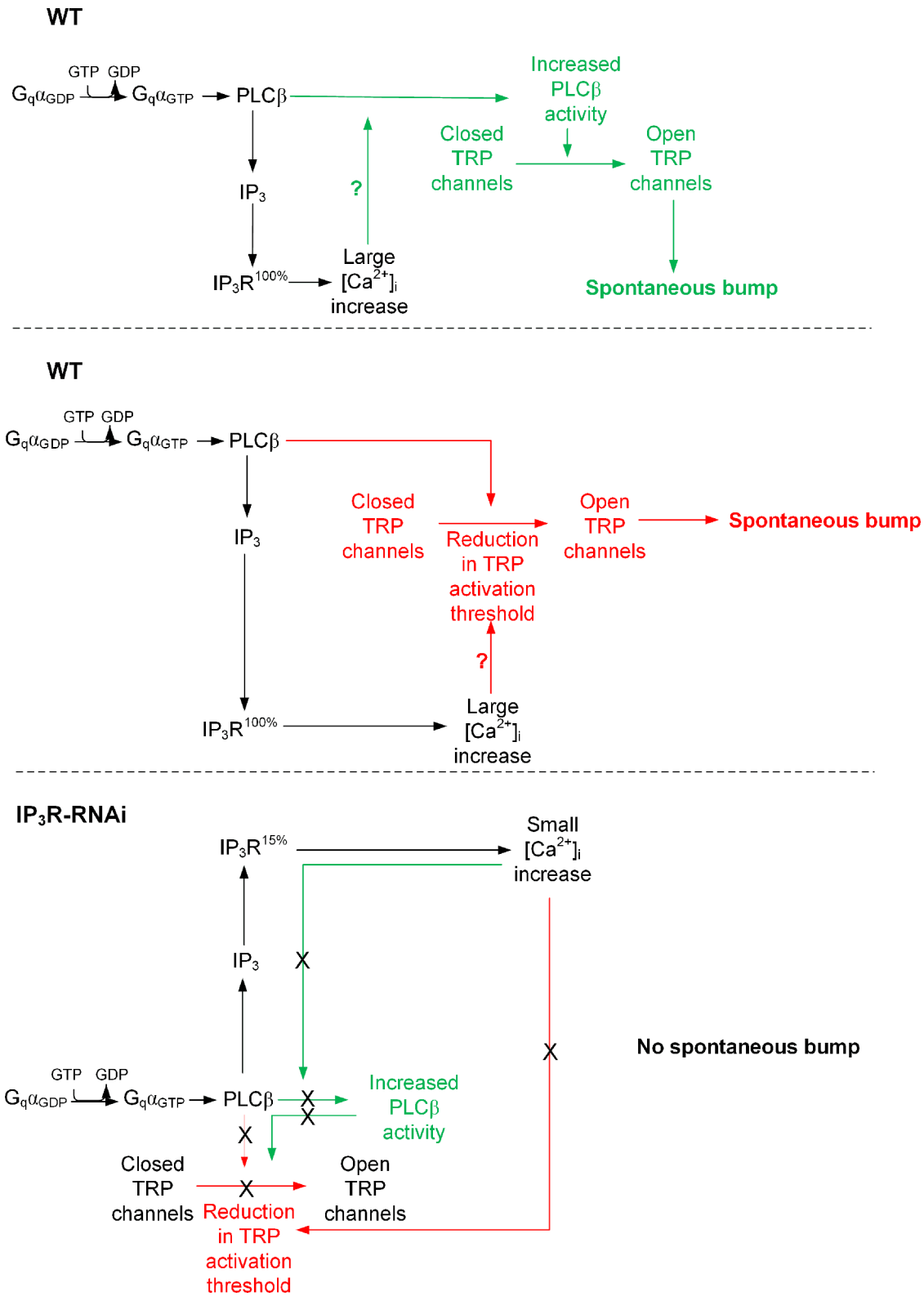

Figure 8. A model explaining the mechanism of spontaneous bump generation and the effect of reduced IP_3R level and Ca^{2+} release on spontaneous bump generation (see Discussion).

results in hydrolysis of PIP_2 producing IP_3 (Fig. 8, black parts of the scheme). Since there are no IP_3 buffers in the microvilli and the IP_3 degradation time is relatively slow (~1 s; Allbritton et al., 1992), the produced IP_3 molecules diffuse fast along the microvillus at an estimated time of ~1 ms along 1 μm long microvillus (Fig. 9*A*,*B*; Allbritton et al., 1992) and bind to IP_3R located at the nearby submicrovillar cisternae (SMC; the photoreceptors' extensions of smooth ER; Fig. 9). IP_3R channels residing at the SMC (Raghu et al., 2000), which are large channels with high sensitivity for IP_3 (Foskett et al., 2007) and thus can be activated at low PLCβ activity (Dickson et al., 2013), open and release Ca^{2+} juxtaposed to the base of the microvillus. The released Ca^{2+} steeply raises the

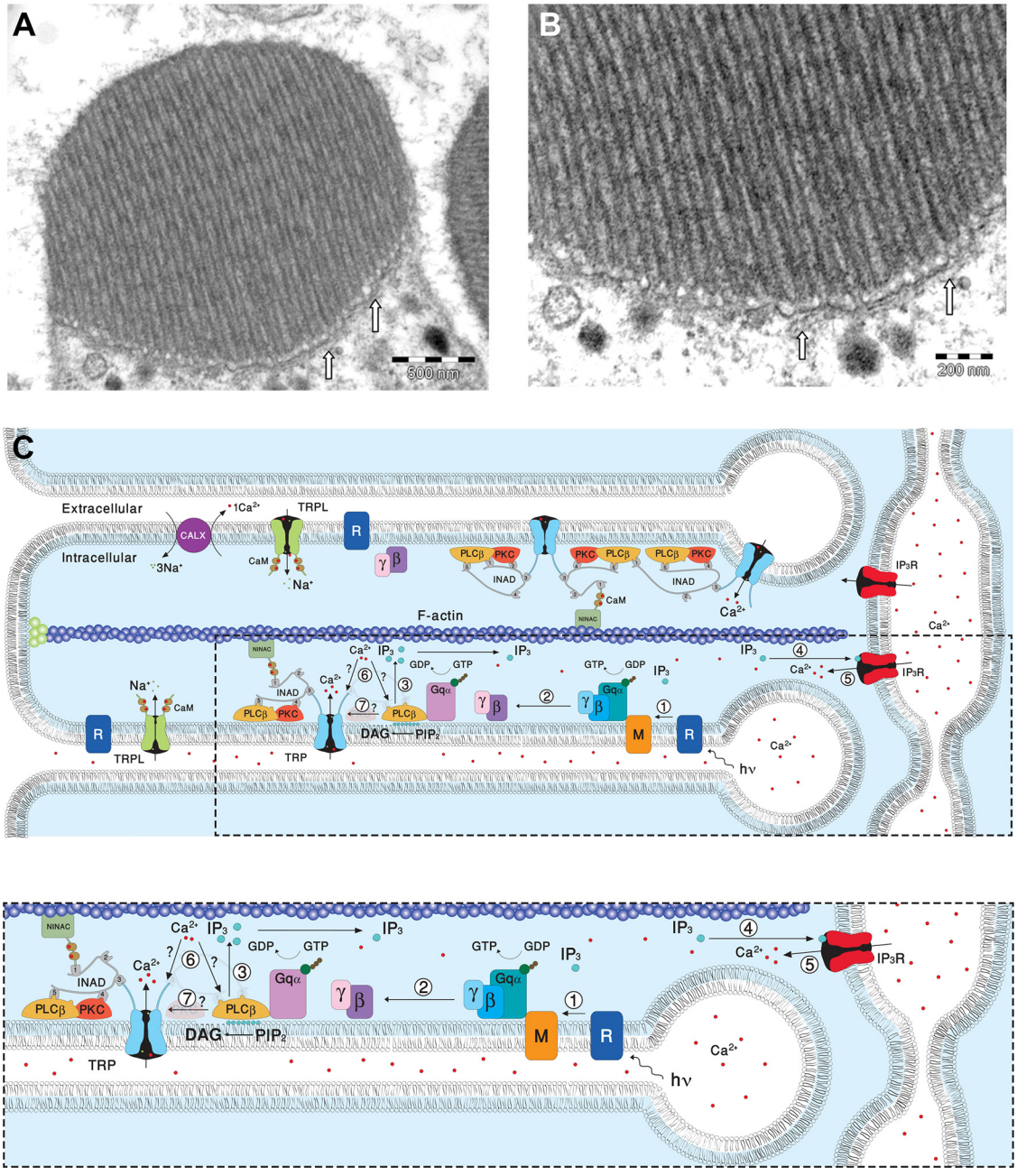

Figure 9. EM pictures and a diagram showing structural features of the signaling compartment and the localization of the signaling molecules. Top, TEM showing the microvilli composing dark-adapted WT rhabdomere. ***A***, TEM of a cross section of a rhabdomere, which is composed of tightly packed microvilli. The elongated membrane vesicles virtually touching the base of the microvilli (arrows) are extensions of the smooth ER called SMC and constitute the IP_3-sensitive Ca^{2+} stores. ***B***, Higher magnification of the rhabdomere at the base of the microvilli, showing the SMC (arrows). ***C***, A diagram showing the molecular components of the signal transduction cascade of *Drosophila*:,1, Upon absorption of a photon ($h\nu$), rhodopsin (R) is converted into metarhodopsin (M). 2, The R-to-M photoconversion leads to the activation of heterotrimeric G-protein($G_q\alpha,\beta,\gamma$) by promoting the GDP-to-GTP exchange. 3, The GDP-to-GTP exchange in turn leads to activation of PLCβ, which hydrolyzes PIP_2 into the soluble IP_3 and the membrane-bound DAG. 4, Subsequently, IP_3 molecules (blue dots) diffuse along the microvillus and bind to the IP_3 receptor (IP_3R) located at the SMC. 5, Binding of IP_3 to the IP_3R causes release of Ca^{2+} (red dots) from the SMC and its diffusion back into the microvillus followed by binding of Ca^{2+} to both PLCβ and the TRP channel. 6, This binding either facilitates the catalytic activity of PLCβ (?) or reduces the threshold of TRP channel activation (?, see Fig. 8). 7, Two classes of light-sensitive channels, the TRP and TRPL, open by a still unknown mechanism (?) following PLCβ activation. The TRP and TRPL channel openings lead to elevation of cellular Ca^{2+}. Elevation of DAG and Ca^{2+} promote eye-specific PKC activity, which regulates channel activity. PLCβ, PKC, and the TRP ion channel form a supramolecular complex with the scaffolding protein INAD, which is bound to the F-actin cytoskeleton via the NINAC protein. Bottom, Magnification of the box marked by dotted lines in the top diagram.

local Ca^{2+} concentration, probably to the μM range, because of the very small aqueous volume of the microvillus (Fig. 9; Postma et al., 1999) and the relatively large local Ca^{2+} elevation via the release mechanism. Accordingly, a single IP_3R channel can release $\sim 10^4$ Ca^{2+} ions in 1 ms channel opening (Bezprozvanny and Ehrlich, 1994) and Ca^{2+}-induced Ca^{2+} release mechanism is a property of the IP_3R channels and of the ryanodine receptors, which reside in the ER (Walz et al., 1995; Arnon et al., 1997). Ca^{2+} released via IP_3R of the WT SMC diffuse back toward the activated PLCβ and the TRP/TRPL channels in the microvillus (Figs. 8, green and red upper pointing arrows, 9). Although Ca^{2+} diffuses ~20-fold slower than IP_3 due to strong buffering (All-

britton et al., 1992), the diffusion constant strongly depends on Ca^{2+} concentration. Accordingly, at ~250 μM the Ca^{2+} diffusion coefficient is as large as that of IP_3 (Allbritton et al., 1992). Once a single TRP channel is activated, the large Ca^{2+} influx through this channel is sufficient to facilitate the rest of the active PLCβ molecules (Fig. 8, green scheme) or reduce the threshold for TRP/TRPL channel activation in this microvillus (Fig. 8, red scheme) and produce a bump that reflects activation of the entire microvillus (Hamdorf and Kirschfeld, 1980; Postma et al., 1999). When there is abnormally low Ca^{2+} release via the IP_3R because of low IP_3R expression levels (IP_3R-RNAi), there is not enough Ca^{2+} to increase PLC activity (Fig. 8, bottom green scheme) or to reduce TRP activation threshold (Fig. 8, bottom red scheme), and activated PLC in this microvillus does not produce a bump, leading to abnormally low frequency of dark bumps (Fig. 8, bottom scheme).

Why previous studies failed to observe any phenotype in photoreceptors lacking the IP_3R

The invasive whole-cell recording technique, which was used in previous studies and avoided Ca^{2+} buffering of the pipette solution, most likely resulted in abnormally elevated cytosolic Ca^{2+} concentration, which also allowed the Ca^{2+} pump to keep the stores full. This artificially elevated cytosolic [Ca^{2+}] together with the constitutive Ca^{2+} leak from the full stores, bypassed the need to mobilize Ca^{2+} via functional IP_3R to facilitate PLCβ activity and reach its critical catalytic activity level needed to activate the TRP/TRPL channels. In the present study in the intact eye, a significant reduction in light-response amplitude was observed when the IP_3R level was reduced. Furthermore, when cellular [Ca^{2+}] was reduced by prolonged extracellular EGTA application, the light response of the IP_3R-deficient flies was further suppressed. Moreover, when using invasive patch-clamp whole-cell recordings without Ca^{2+} buffering of the pipette solution, no significant difference between WT and IP_3R-deficient flies was observed, as found in the previous study. However, when pipette Ca^{2+} was reduced with EGTA, the phenotype of reduced light excitation was observed in both reduced quantum-bump frequency as well as in macroscopic light-response suppression. Unlike quantum bumps, dark bumps were virtually eliminated even without buffering the pipette Ca^{2+} in IP_3R-deficient flies, indicating that in the dark the IP_3R-deficiency led to abnormally low cytosolic [Ca^{2+}], possibly due to reduced Ca^{2+} leak from stores leading to cellular [Ca^{2+}] below the critical level required for PLC activation observed in WT flies. Alternatively, the positive feedback between the released Ca^{2+} and PLC may function at single PLC molecules. Hence the nominal pipette Ca^{2+} is not sufficient to allow PLC activity to pass the threshold of channel activation, but the released Ca^{2+} via IP_3R activation together with pipette Ca^{2+} allows PLC activity to pass this threshold and generate dark-bump.

Implications on IP signaling in general

There is a striking functional similarity between, the cerebellar Purkinje cell (PC) proteins of the IP signaling and *Drosophila* photoreceptors (Hartmann et al., 2008), but the link of cerebellar mGluR1 receptor to TRPC3 activation is not clear. Interestingly, in PC neurons, stromal interaction molecule 1 (STIM1) was proved an essential regulator of Ca^{2+} level in neuronal endoplasmic reticulum Ca^{2+} stores. Accordingly, STIM1-specific deletion caused impairments in slow synaptic current and cerebellar motor behavior. Strikingly, refilling empty Ca^{2+} stores through increased Ca^{2+} level in the cytosol partially rescued the phenotype of the *stim1* knock-out mice (Hartmann et al., 2014), reminiscent of the rescue of the phenotype of the IP_3R-deficient fly by artificially elevated cytosolic Ca^{2+}. Thus, the facilitatory role of released Ca^{2+} on PLC in light excitation of *Drosophila* photoreceptors represents an essential mechanism that operates in other PI systems.

References

Abramoff MD, Magelhaes PJ, Ram SJ (2004) Image processing with ImageJ. Biophotonics Int 11:36–42.

Acharya JK, Jalink K, Hardy RW, Hartenstein V, Zuker CS (1997) InsP3 receptor is essential for growth and differentiation but not for vision in *Drosophila*. Neuron 18:881–887. CrossRef Medline

Agam K, von Campenhausen M, Levy S, Ben-Ami HC, Cook B, Kirschfeld K, Minke B (2000) Metabolic stress reversibly activates the *Drosophila* light-sensitive channels TRP and TRPL *in vivo*. J Neurosci 20:5748–5755. Medline

Agam K, Frechter S, Minke B (2004) Activation of the *Drosophila* TRP and TRPL channels requires both Ca^{2+} and protein dephosphorylation. Cell Calcium 35:87–105. CrossRef Medline

Allbritton NL, Meyer T, Stryer L (1992) Range of messenger action of calcium ion and inositol 1,4,5-trisphosphate. Science 258:1812–1815. CrossRef Medline

Arnon A, Cook B, Montell C, Selinger Z, Minke B (1997) Calmodulin regulation of calcium stores in phototransduction of *Drosophila*. Science 275:1119–1121. CrossRef Medline

Barash S, Minke B (1994) Is the receptor potential of fly photoreceptors a summation of single-photon responses? Comments Theor Biol 3:229–263.

Berridge MJ (1993) Inositol trisphosphate and calcium signalling. Nature 361:315–325. CrossRef Medline

Berridge MJ, Lipp P, Bootman MD (2000) The versatility and universality of calcium signalling. Nat Rev Mol Cell Biol 1:11–21. CrossRef Medline

Bezprozvanny I, Ehrlich BE (1994) Inositol (1,4,5)-trisphosphate ($InsP_3$)-gated Ca channels from cerebellum: conduction properties for divalent cations and regulation by intraluminal calcium. J Gen Physiol 104:821–856. CrossRef Medline

Chen TW, Wardill TJ, Sun Y, Pulver SR, Renninger SL, Baohan A, Schreiter ER, Kerr RA, Orger MB, Jayaraman V, Looger LL, Svoboda K, Kim DS (2013) Ultrasensitive fluorescent proteins for imaging neuronal activity. Nature 499:295–300. CrossRef Medline

Chorna-Ornan I, Tzarfaty V, Ankri-Eliahoo G, Joel-Almagor T, Meyer NE, Huber A, Payre F, Minke B (2005) Light-regulated interaction of Dmoesin with TRP and TRPL channels is required for maintenance of photoreceptors. J Cell Biol 171:143–152. CrossRef Medline

Chu B, Liu CH, Sengupta S, Gupta A, Raghu P, Hardie RC (2013) Common mechanisms regulating dark noise and quantum bump amplification in *Drosophila* photoreceptors. J Neurophysiol 109:2044–2055. CrossRef Medline

Chyb S, Raghu P, Hardie RC (1999) Polyunsaturated fatty acids activate the *Drosophila* light-sensitive channels TRP and TRPL. Nature 397:255–259. CrossRef Medline

Cook B, Minke B (1999) TRP and calcium stores in *Drosophila* phototransduction. Cell Calcium 25:161–171. CrossRef Medline

Cook B, Bar-Yaacov M, Cohen-Ben AH, Goldstein RE, Paroush Z, Selinger Z, Minke B (2000) Phospholipase C and termination of G-protein-mediated signalling in vivo. Nat Cell Biol 2:296–301. CrossRef Medline

Delgado R, Muñoz Y, Peña-Cortés H, Giavalisco P, Bacigalupo J (2014) Diacylglycerol activates the light-dependent channel TRP in the photosensitive microvilli of *Drosophila* melanogaster photoreceptors. J Neurosci 34:6679–6686. CrossRef Medline

Devary O, Heichal O, Blumenfeld A, Cassel D, Suss E, Barash S, Rubinstein CT, Minke B, Selinger Z (1987) Coupling of photoexcited rhodopsin to inositol phospholipid hydrolysis in fly photoreceptors. Proc Natl Acad Sci U S A 84:6939–6943. CrossRef Medline

Dickson EJ, Falkenburger BH, Hille B (2013) Quantitative properties and receptor reserve of the IP(3) and calcium branch of G(q)-coupled receptor signaling. J Gen Physiol 141:521–535. CrossRef Medline

Elia N, Frechter S, Gedi Y, Minke B, Selinger Z (2005) Excess of Gbetae over Gqalphae in vivo prevents dark, spontaneous activity of *Drosophila* photoreceptors. J Cell Biol 171:517–526. CrossRef Medline

Essen LO, Perisic O, Katan M, Wu Y, Roberts MF, Williams RL (1997) Structural mapping of the catalytic mechanism for a mammalian

phosphoinositide-specific phospholipase C. Biochemistry 36:1704–1718. CrossRef Medline

Foskett JK, White C, Cheung KH, Mak DO (2007) Inositol trisphosphate receptor Ca^{2+} release channels. Physiol Rev 87:593–658. CrossRef Medline

Hamdorf K, Kirschfeld K (1980) Reversible events in the transduction process of photoreceptors. Nature 283:859–860. CrossRef Medline

Hardie RC (1995a) Effects of intracellular Ca^{2+} chelation on the light response in *Drosophila* photoreceptors. J Comp Physiol A 177:707–721. CrossRef Medline

Hardie RC (1995b) Photolysis of caged Ca^{2+} facilitates and inactivates but does not directly excite light-sensitive channels in *Drosophila* photoreceptors. J Neurosci 15:889–902. Medline

Hardie RC (1996a) INDO-1 measurements of absolute resting and light-induced Ca^{2+} concentration in *Drosophila* photoreceptors. J Neurosci 16:2924–2933. Medline

Hardie RC (1996b) A quantitative estimate of the maximum amount of light-induced Ca^{2+}release in *Drosophila* photoreceptors. J Photochem Photobiol B 35:83–89. CrossRef Medline

Hardie RC, Minke B (1992) The trp gene is essential for a light-activated Ca^{2+} channel in *Drosophila* photoreceptors. Neuron 8:643–651. CrossRef Medline

Hardie RC, Postma M (2008) Phototransduction in microvillar photoreceptors of *Drosophila* and other invertebrates. In: The senses: a comprehensive reference (Allan IB, Akimichi K, Gordon MS, Gerald W, Thomas DA, Richard HM, Peter D, Donata O, Stuart F, Gary KB, Bushnell MC, Jon HK, Esther G, eds), pp 77–130. New York: Academic.

Hardie RC, Martin F, Cochrane GW, Juusola M, Georgiev P, Raghu P (2002) Molecular basis of amplification in *Drosophila* phototransduction. Roles for G protein, phospholipase C, and diacylglycerol kinase. Neuron 36: 689–701. CrossRef Medline

Hartmann J, Dragicevic E, Adelsberger H, Henning HA, Sumser M, Abramowitz J, Blum R, Dietrich A, Freichel M, Flockerzi V, Birnbaumer L, Konnerth A (2008) TRPC3 channels are required for synaptic transmission and motor coordination. Neuron 59:392–398. CrossRef Medline

Hartmann J, Karl RM, Alexander RP, Adelsberger H, Brill MS, Rühlmann C, Ansel A, Sakimura K, Baba Y, Kurosaki T, Misgeld T, Konnerth A (2014) STIM1 controls neuronal Ca^{2+} signaling, mGluR1-dependent synaptic transmission, and cerebellar motor behavior. Neuron 82:635–644. CrossRef Medline

Henderson SR, Reuss H, Hardie RC (2000) Single photon responses in *Drosophila* photoreceptors and their regulation by Ca 2+. J Physiol 524:179–194. CrossRef Medline

Hofmann T, Obukhov AG, Schaefer M, Harteneck C, Gudermann T, Schultz G (1999) Direct activation of human TRPC6 and TRPC3 channels by diacylglycerol. Nature 397:259–263. CrossRef Medline

Katz B, Minke B (2009) *Drosophila* photoreceptors and signaling mechanisms. Front Cell Neurosci 3:2. CrossRef Medline

Katz B, Minke B (2012) Phospholipase C-mediated suppression of dark noise enables single-photon detection in *Drosophila* photoreceptors. J Neurosci 32:2722–2733. CrossRef Medline

Mealey-Ferrara ML, Montalvo AG, Hall JC (2003) Effects of combining a cryptochrome mutation with other visual-system variants on entrainment of locomotor and adult-emergence rhythms in *Drosophila*. J Neurogenet 17:171–221. CrossRef Medline

Minke B (2012) The history of the prolonged depolarizing afterpotential (PDA) and its role in genetic dissection of *Drosophila* phototransduction. J Neurogenet 26:106–117. CrossRef Medline

Minke B, Cook B (2002) TRP channel proteins and signal transduction. Physiol Rev 82:429–472. Medline

Minke B, Selinger Z (1992) The inositol-lipid pathway is necessary for light excitation in fly photoreceptors. In: Sensory transduction (Corey D, Roper SD, eds), pp 202–217. New York: Rockefeller UP.

Montell C (1999) Visual transduction in *Drosophila*. Annu Rev Cell Dev Biol 15:231–268. CrossRef Medline

Montell C, Rubin GM (1989) Molecular characterization of the *Drosophila* trp locus: a putative integral membrane protein required for phototransduction. Neuron 2:1313–1323. CrossRef Medline

Niemeyer BA, Suzuki E, Scott K, Jalink K, Zuker CS (1996) The *Drosophila* light-activated conductance is composed of the two channels TRP and TRPL. Cell 85:651–659. CrossRef Medline

Pak WL, Leung HT (2003) Genetic approaches to visual transduction in *Drosophila* melanogaster. Receptors Channels 9:149–167. CrossRef Medline

Parnas M, Katz B, Minke B (2007) Open channel block by Ca^{2+} underlies the voltage dependence of *Drosophila* TRPL channel. J Gen Physiol 129: 17–28. CrossRef Medline

Patton C, Thompson S, Epel D (2004) Some precautions in using chelators to buffer metals in biological solutions. Cell Calcium 35:427–431. CrossRef Medline

Peretz A, Sandler C, Kirschfeld K, Hardie RC, Minke B (1994a) Genetic dissection of light-induced Ca^{2+} influx into *Drosophila* photoreceptors. J Gen Physiol 104:1057–1077. CrossRef Medline

Peretz A, Suss-Toby E, Rom-Glas A, Arnon A, Payne R, Minke B (1994b) The light response of *Drosophila* photoreceptors is accompanied by an increase in cellular calcium: effects of specific mutations. Neuron 12: 1257–1267. CrossRef Medline

Phillips AM, Bull A, Kelly LE (1992) Identification of a *Drosophila* gene encoding a calmodulin-binding protein with homology to the trp phototransduction gene. Neuron 8:631–642. CrossRef Medline

Postma M, Oberwinkler J, Stavenga DG (1999) Does Ca^{2+} reach millimolar concentrations after single photon absorption in *Drosophila* photoreceptor microvilli? Biophys J 77:1811–1823. CrossRef Medline

Raghu P, Colley NJ, Webel R, James T, Hasan G, Danin M, Selinger Z, Hardie RC (2000) Normal phototransduction in *Drosophila* photoreceptors lacking an InsP3 receptor gene. Mol Cell Neurosci 15:429–445. CrossRef Medline

Ranganathan R, Bacskai BJ, Tsien RY, Zuker CS (1994) Cytosolic calcium transients: spatial localization and role in *Drosophila* photoreceptor cell function. Neuron 13:837–848. CrossRef Medline

Rubinstein CT, Bar-Nachum S, Selinger Z, Minke B (1989) Chemically-induced retinal degeneration in rdgB (retinal degeneration B) mutant of *Drosophila*. Vis Neurosci 2:541–551. CrossRef Medline

Srikanth S, Wang Z, Tu H, Nair S, Mathew MK, Hasan G, Bezprozvanny I (2004) Functional properties of the *Drosophila* melanogaster inositol 1,4,5-trisphosphate receptor mutants. Biophys J 86:3634–3646. CrossRef Medline

Taylor CW, Tovey SC (2010) IP_3 receptors: toward understanding their activation. Cold Spring Harb Perspect Biol 2:a004010. CrossRef Medline

Walz B, Baumann O, Zimmermann B, Ciriacy-Wantrup EV (1995) Caffeine- and ryanodine-sensitive Ca 2+-induced Ca^{2+} release from the endoplasmic reticulum in honeybee photoreceptors. J Gen Physiol 105: 537–567. CrossRef Medline

Wang T, Xu H, Oberwinkler J, Gu Y, Hardie RC, Montell C (2005) Light activation, adaptation, and cell survival functions of the Na^{+}/Ca^{2+} exchanger CalX. Neuron 45:367–378. CrossRef Medline

Weiss S, Kohn E, Dadon D, Katz B, Peters M, Lebendiker M, Kosloff M, Colley NJ, Minke B (2012) Compartmentalization and Ca^{2+} buffering are essential for prevention of light-induced retinal degeneration. J Neurosci 32:14696–14708. CrossRef Medline

Wong F, Knight BW, Dodge FA (1982) Adapting bump model for ventral photoreceptors of Limulus. J Gen Physiol 79:1089–1113. CrossRef Medline

Wu CF, Pak WL (1975) Quantal basis of photoreceptor spectral sensitivity of *Drosophila* melanogaster. J Gen Physiol 66:149–168. CrossRef Medline

Yoon J, Leung HT, Lee S, Geng C, Kim Y, Baek K, Pak WL (2004) Specific molecular alterations in the norpA-encoded phospholipase C of *Drosophila* and their effects on electrophysiological responses in vivo. J Neurochem 89:998–1008. CrossRef Medline